High selenium in the Carboniferous Coal Measures of Northumberland, North East England

Liam A. Bullock[a,*], John Parnell[a], Magali Perez[b], Joseph G. Armstrong[a], Joerg Feldmann[b], Adrian J. Boyce[c]

[a] *School of Geosciences, University of Aberdeen, Aberdeen AB24 3UE, UK*
[b] *Trace Element Speciation Laboratory (TESLA), Department of Chemistry, University of Aberdeen, Aberdeen AB24 3UE, UK*
[c] *Scottish Universities Environmental Research Centre, East Kilbride, Glasgow, UK*

ABSTRACT

The Carboniferous Lower and Middle Coal Measures coals of the Northumberland Coalfield are anomalously rich in selenium (Se) content (up to 62 ppm) compared to the averages for the common UK and worldwide coals. As well as posing an environmental toxicity threat, Se is now regarded as an important resource for alloys, photovoltaic products and nanotechnologies, and high Se coals in North East England offer an opportunity to assess the Se means of occurrence, origins, transport mechanisms and enrichment in coals. At least two generations of pyrite host high Se in the sampled coal seams: microbial-formed disseminated pyrite (both cubic and framboidal in habit) and later cleat-filling pyrite, identified by petrographic observations, laser ablation methods and sulphur isotope compositions. There is a notable Se enrichment of up to 250 ppm in later formed cleat-filling pyrite. Trace element enrichment may have been sourced and influenced by seawater distribution during diagenesis, and localised dykes and deformation may have acted as an enrichment mechanism for sampled seams in the region. The high Se coals in Northumberland may provide a potential E tech element source and should be considered and carefully managed as coal mining and production are reduced in the area. The study also highlights the nature of Se enrichment in pyritic coals affected by cleat formation and multiple episodes of mineralisation, important as critical element demand continues to increase worldwide.

1. Introduction

Improved understanding of the concentration and spatial distribution of critical elements such as selenium (Se) in coals is economically important, particularly as the worldwide demand for viable sources of Se continues to grow. The Carboniferous-aged coals in the Northumberland Coalfield (North East England) have been previously shown to contain high pyrite (of multiple generations) and sulphur (S), important for resource development and utilisation (Turner and Richardson, 2004). High-S coals may contain high Se (Coleman et al., 1993), as Se and S share chemical affinities and substitute readily in pyrite (Emsbo et al., 2003; Pals et al., 2003; Yudovich and Ketris, 2006; Tanner et al., 2016; Keith et al., 2017). Multiple generations of pyrite formation in coals may also enrich Se content of coals (e.g. Ayrshire coals; Bullock et al., 2018b).

Sedimentary settings where Se enrichment is typically evident include organic and pyritic coals and black shales (Clark et al., 1980; Mao et al., 1988; Dreher and Finkelman, 1992; Zheng et al., 1992; Coleman et al., 1993; He et al., 2002; Lemly, 2004; Liu et al., 2006; Yudovich and Ketris, 2006; Li and Zhao, 2007; Ketris and Yudovich, 2009; Dai et al., 2015a, 2015b, 2017; Diehl et al., 2012; Lei, 2012; Zhu et al., 2012; Pazand, 2015; Parnell et al., 2016, 2018a; Armstrong et al., 2018; Bullock et al., 2018a, 2018b), red bed sediments (Hofmann, 1991; Parnell et al., 2016, 2018b; Spinks et al., 2014, 2016) or sandstone-hosted roll-type uranium deposits (Harshman, 1966; Howard, 1977; Granger and Warren, 1978; Reynolds and Goldhaber, 1983; Min et al., 2005; Abzalov, 2012; Dai et al., 2015a; Bullock and Parnell, 2017). Selenium is mobilised under oxidising conditions (Howard, 1977; Northrop and Goldhaber, 1990; Simon et al., 1997; Xiong, 2003; Min et al., 2005; Spinks et al., 2014, 2016), and may be precipitated and immobilised in the presence of a reducing agent (e.g. carbonaceous materials, sulphides, biogenic H_2S, ferromagnesian minerals; Spinks et al., 2014, 2016). In continental sandstone settings, Se may be co-precipitated with iron oxides and adsorbed from solution (Parnell et al., 2018b). Selenium is often accompanied by high V, Cr, Mo, U and Te (Yudovich and Ketris, 2006; Dai et al., 2015a; Bullock and Parnell,

2017).

The average Se content for UK and worldwide coals are 1.8 and 1.3 ppm respectively (Spears and Zheng, 1999; Ketris and Yudovich, 2009; Yudovich and Ketris, 2015). Selenium is considered a coalphile element, with a strong affinity to organic and inorganic (e.g. sulphides) coal matter, similar to elements such as Ge and S (Yudovich and Ketris, 2006). Inorganically associated Se in coal typically occurs in association with pyrite and may also occur in association with rare clausthalite (PbSe), ferroselite ($FeSe_2$), galena (PbS), and clays (Finkelman et al., 1979; Finkelman, 1980; Swaine, 1990; Goodarzi and Swaine, 1993; Hower and Robertson, 2003; Dai et al., 2006, 2008; Li and Zhao, 2007). Metalliferous enrichment in coal may occur during peat accumulation, during diagenesis, or by epigenesis (Seredin and Finkelman, 2008; Dai et al., 2015b; Bullock et al., 2018b). In reducing coal-forming environments, Se concentrates in syngenetic or epigenetic sulphide phases, while in oxidising environments, Se is enriched in bed oxidation zones (closely associated with precipitation of U, Fe, Mo, V and Pb; Yudovich and Ketris, 2006). Elevated Se (and other associated trace elements) in coals may also be attributed to input from sediment source regions and percolating solutions (e.g. the Yili coals of Xinjiang, northwestern China; Dai et al., 2015a).

Over recent years, Se has become an increasingly important 'E tech' element, used in alloys, photovoltaic products and nanotechnologies (Jin et al., 2016; Wei et al., 2016), and coal has been specifically identified as a promising source for future resources (Seredin and Finkelman, 2008; UKERC, 2012; Seredin et al., 2013; Dai and Finkelman, 2018; Yang et al., 2018). Pyrite has also been noted as a potential economic source of Se (Keith et al., 2017). As well as economic benefits, trace elements such as Se have the potential for release into the environment from coal utilisation and combustion (Lakin and Davidson, 1973; Swaine, 1990). High Se coals may pose an environmental threat to air quality (coal combustion), and to local soils, surface and groundwater systems (Agnihotri et al., 1998; McDonald and Strosher, 1998; Lemly, 2004; Dai et al., 2012; Hendry et al., 2015). Therefore, sites of potentially high pyritic and S content with ongoing coal mining operations, such as in areas of Northumberland, northeast England (Fig. 1), warrant attention for their Se in coal potential. Identification of high Se in pyritic coals is essential for future advances and decisions in E tech development, coal processing and site management. While coals are not currently considered a viable source of Se compared to more conventional extractable deposits (e.g. by-product recovery of Cu processing; Brown, 2000; Plant et al., 2013), its presence in high abundances may prove an important by-product in regions where coal processing is winding down (such as historically extensive coal-producing areas of the UK), and as methods of critical element extraction continue to improve globally. This is particularly significant as demand for Se increases, while worldwide conventional Se-hosting deposits are exhausted. Coals with potential economic significance for critical elements, with concentrations in coal at least 10-times higher than the respective averages for world coals (Seredin and Finkelman, 2008), have been termed 'coal-hosted rare-metal deposits' (Dai and Finkelman, 2018) or 'metalliferous coals' (Seredin and Finkelman, 2008). As demand increases for critical elements such as Se, it is important to identify regions of metalliferous coals.

Existing Se data from Northumberland coals are limited, with concentrations of 16 bituminous coals available in the world coal database of Bragg et al. (1998). This Northumberland sample set gives an average of 3.4 ppm, higher than the averages for the common UK and world coals. These 16 coals were all sampled at the Ellington coal mine, near Lynemouth (Fig. 1). The sample set includes an anomalous Se value of 15 ppm, taken from the Brass Thill coal bed, which contains pyrite and ankerite (Bragg et al., 1998). This suggests that pyritic Northumberland coals may contain anomalously high Se, meriting further investigation. This paper aims to describe Se concentrations in six seams from the Northumberland Coalfield to determine the means of mineralogical occurrence, the source of abundant Se in the sampled coals, the economic viability of the region and to compare Northumberland coals to other recorded Se-bearing coals, both locally and worldwide. The origin of pyrite, Se occurrence, source and transport mechanisms will also be assessed, and the future importance of this resource will be discussed. The Shotton Surface Mine (Cramlington) was chosen as the main sample site due to the ongoing coal mining and processing operations, and the exposure of multiple seams, including pyritic coals. Three other localities were sampled and measured for a local comparison, and studies of worldwide Se-bearing coals were included for a global comparison. Results have important implications for Se-bearing coals as a potential semi-metal resource, particularly as means of extraction continue to improve. Though high Se in selected seam samples do not apply to the full extent of the Northumberland Coalfield, the identification of particularly enriched seams and strata in the region allows us to pinpoint Se targets and potential means of enrichment that could affect other seams locally, regionally or indeed worldwide.
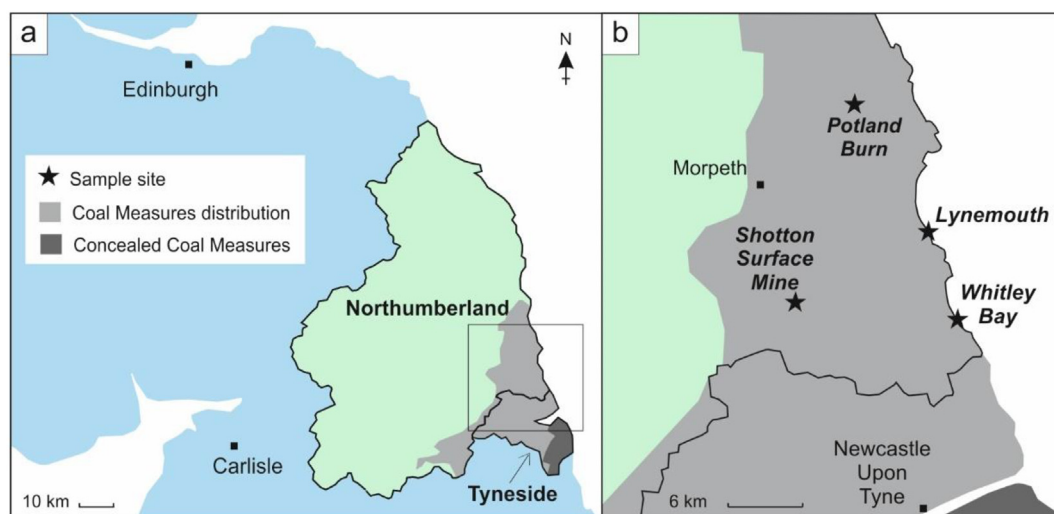

Fig. 1. The county of Northumberland (with the conurbation of Tyneside to the south) in North East England (a) and study sample sites in South East Northumberland (b). Coal Measures distribution and concealed Coal Measures also shown for Northumberland and Tyneside (after Bloodworth et al., 2000).

2. Geological setting and study site

A detailed overview of the geological history of the greater Northumberland region is provided in Turner and Richardson (2004) and is summarised here. The Northumberland Coalfield forms part of the Carboniferous Coal Measures of the UK, bordered to the southwest by Carboniferous Yordale Group, which hosts extensive mineral veins of the North Pennine Orefield and the Weardale Granite (Mills and Holliday, 1998; Turner and Richardson, 2004), and to the south by the Permian Zechstein Group. Only the Lower and Middle Coal Measures (Westphalian A, B and part of C) are preserved in Northumberland (Fig. 1). These Coal Measures comprise a 750 m-thick alluvial succession, deposited on a low-lying coastal alluvial plain and more marine-influenced environments to the south and southwest. The region (including the Shotton site) is typically rifted and faulted, trending E-W, formed during the early to mid-Carboniferous phase of subsidence and sedimentation, followed by the late Dinantian to Westphalian post-rift thermal subsidence phase (Leeder and McMahon, 1988; Turner and Richardson, 2004). The Shotton site is also cut by a number of small exposed and subsurface microgabbroic Palaeogene dykes.

Northumberland has an extensive history of coal mining, with activity as far back as 1236 (National Coal Board Archive, 2011). There are still operational opencast sites in the county, including Shotton and Potland Burn Surface Mines (the latter recently completed coaling in 2016), and Coal Measures are exposed at coastal sections of Lynemouth and Whitley Bay (Fig. 1). The 400 ha Shotton site (Fig. 2), currently operated by Banks Group, is located to the west of Cramlington and north of Newcastle upon Tyne. As of May 2018, the site mines coal, shale and fireclay. Though the site is active (planned activity up to 2019), there are plans to wind down production and restore the site to agricultural, woodland, nature conservation and amenity uses by 2021 (Banks Group, 2018). Coal production is used for electricity generation at Lynemouth Power Station (Ashington, Northumberland), and Drax Power Station (North Yorkshire), as well as being sold for domestic use. Previously worked and currently exposed seams at the Shotton site include several from the Middle Coal Measures (Top Durham Low Main, Durham Low Main, Northumberland Low Main, Top Plessey (Top Leaf and Bottom Leaf), Plessey and Bottom Plessey) and the Lower Coal Measures (Beaumont, Hodge, Top Tilley, Bottom Tilley, Top Busty, Middle Busty and Bottom Busty; Fig. 2).

3. Methods

Sub-sample seam picks were collected in-situ from exposed (surface) seams at the Shotton site. Though pyritic samples were selected where evident, the aim was to collect unweathered samples from each seam that provide a representative overview. However, to avoid sampling bias that may result from selecting particularly mineralised samples (e.g. pyritic coals), generalised coal properties from cored samples (taken by Banks Group) are provided in Table 1 to give a representative summary of sampled coal seams.

Whole rock samples from exposed seams (Durham Low Main, Northumberland Low Main, Top Plessey, Plessey, Bottom Plessey, Top Busty and Bottom Busty) were analysed by inductively coupled plasma-mass spectrometry (ICP-MS) for determination of selenium (Se) and iron (Fe). Sulphur (S) and total organic carbon (TOC) were measured to a precision of ± 0.5% using a LECO CS225 elemental analyser. Samples were measured both before decarbonation (with no prior treatment for S content) and after decarbonation (for TOC with HCl treatment). Analyses were calibrated and run concurrently with standards 501-024 (Leco Instruments, 3.23 ± 0.03% C, 0.047 ± 0.003% S, instrument uncertainty ± 0.05% C, ± 0.002% S) and BC-CRM 362 (Bureau of Analysed Samples Ltd., 1.48% S). The repeatability of sample results was consistently within 1%, based on the three runs of certified versus obtained values, and methodological interference uncertainty was determined and corrected based on the results of three blanks. Resulting

trace S and TOC values obtained for standard and blank samples were algebraically subtracted from sample responses to avoid analytical interferences. Select regional coals from Whitley Bay, Potland Burn and Lynemouth (Fig. 1) were also analysed for Se, S, Fe and TOC for a regional comparison, and Se content of Carboniferous coals was measured in samples from across British Coalfields for a wider comparison (Bullock et al., 2018a).

Northumberland coal samples were measured by a combination of conventional ICP-MS and ICP-AES, and by the newly developed low Se concentration ICP-MS method of Henn et al. (2018). Each sample was milled and homogenised, with 0.5 g partially digested using aqua regia. Inter-element spectral interferences were accounted for, and standard variabilities for calibration were corrected (standards utilised - MRGeo08 mid-range multi-element standard, GBM908-10 base metal standard, OGGeo08 ore grade multi-element standard and GEOMS-03 multi-element standard). This method represents a partial leach of the coals, with digestion of all phases except silicates. Aqua regia digestion is considered to best represent the seawater depositional component of organic sediments (e.g. black shales; Xu et al., 2012).

Pyrite minerals from select seams were mapped and analysed by laser ablation (LA−) ICP-MS for detailed Se concentrations and zonation within pyrite phases. Laser ablation trace element analysis was performed using a New Wave Research laser ablation system UP 213 nm coupled to an ICP-MS Agilent 7900. Sample mapping was performed at a 10 Hz repetition rate, a spot size of 100 μm and an ablation speed of 50 μm s^{-1}. Each ablation was preceded by 15 s warm up, with a delay of 15 s applied between each ablation. The following isotopes were monitored (dwell time): ^{57}Fe (0.001 s), ^{65}Cu (0.001 s) ^{75}As (0.05 s), ^{78}Se (0.1 s), ^{82}Se (0.1 s), ^{107}Ag (0.1 s), ^{125}Te (0.1 s), ^{126}Te (0.1 s), ^{197}Au (0.1 s), ^{202}Hg (0.1 s), ^{208}Pb (0.05 s) and ^{209}Bi (0.1 s). NIST Glass 612 (NIST Gaithersburg MD) was used to optimise ICP-MS parameters to reach the maximum sensitivity and guarantee a low oxide formation. For that, the ratio ^{232}Th^{16}O$+$/^{232}Th $+$ (as $^{248/232}$) was monitored and maintained below 0.3%. Hydrogen (3.5 ml min^{-1}) was used in the reaction cell to ensure that no interference could affect the Se measurement. Quantification was performed using the reference material MASS-1 Synthetic Polymetal Sulphide (U.S. Geological Survey, Reston, VA). The ratio concentration (μg g^{-1})/counts per second was calculated from the standard MASS-1 and multiplied by the sample counts.

The S isotopic composition of extracted pyrite crystals was determined by conventional S isotopic analyses to provide insights into their origin. Coal samples were partially crushed, and pyrite crystals were hand-picked (free of coal matrix). Pyrite samples were combusted with excess Cu$_2$O at 1075 °C in order to liberate SO$_2$ gas under vacuum conditions. Liberated SO$_2$ gases were analysed on a VG Isotech SIRA II mass spectrometer, with standard corrections applied to raw δ^{66}SO$_2$ values to produce δ^{34}S (^{34}S/^{32}S), with parts per thousand or per mille (‰) variations from the V-CDT standard (Bottrell et al., 1994). Standards utilised were internationally certified reference materials NBS-123 and IAEA-S-3 (supplied by the IAEA) and Scottish Universities Environment Research Centre (SUERC) laboratory standard CP-1, giving 1σ reproducibility, based on repeat analyses, of better than ± 0.2‰.

4. Results

4.1. Sample descriptions

Northumberland coal samples taken from the Shotton site contain three types of pyrite: (1) rare framboidal disseminated pyrite, typically < 5 μm in diameter (Fig. 3a), (2) cubic disseminated pyrite, up to 2 mm in length (Fig. 3b), and (3) pyrite concentrated in cleats, up to 2 mm wide (i.e. fractures, veins and veinlets that resulted from brittle deformation, Fig. 3c). Isolated framboidal and clustered euhedral cubic pyrites are often spatially associated, occurring together, but do not
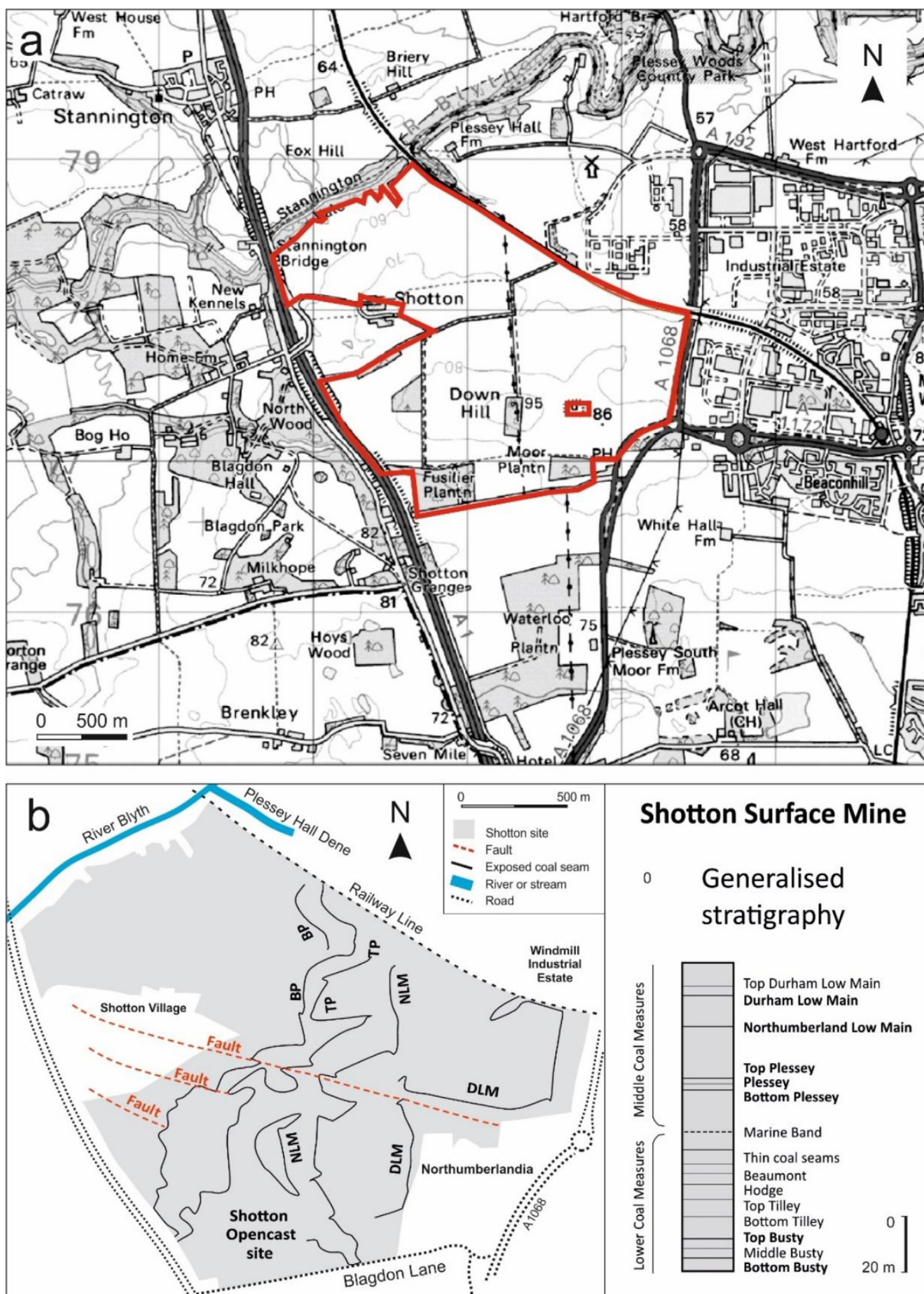
Fig. 2. Shotton site sampling area and generalised coal geology (a) Shotton Surface Mine (red outline), Cramlington, Northumberland, 1:25,000 site location map (Banks Group, 2010; reproduced from Raster 10,000 by permission of Ordinance Survey®); (b) 1:50,000 scale map of the Shotton site and exposed coal seams. Sampled seams (bold text), relative age and stratigraphic position are shown in the generalised vertical section (adapted from Jackson et al., 1985; Banks Group, 2010). (For interpretation of the references to colour in this figure legend, the reader is referred to the web version of this article.)

Table 1

Average overall coal properties for Shotton site coal seams based on borehole samples (2009 coal quality data provided by Banks Group). Coal quality data from phased borehole samples and on an as-received (whole coal) basis.

	Total moisture (%)	Total sulphur (%)	Total volatiles (%)	Total ash (%)
Durham Low Main	No data	No data	No data	No data
Northumberland Low Main	10	0.8	37	7
Top Plessey	8.5	1.1	39.8	21.3
Plessey	8.1	1.5	38.1	9.8
Bottom Plessey	7.7	1.4	40.6	5.4
Top Busty	7.6	0.9	42.2	17.3
Bottom Busty	6.9	1.3	37.9	18.9

define any plane direction. These two pyrite forms are most typical in Durham Low Main, Plessey and Bottom Busty seam samples, distributed sporadically. Cleat-filling pyrite cross-cuts both framboidal and cubic pyrite in Durham Low Main and Top Plessey seam samples. Cleats form intricate networks in coal, and typically follow the plane defined by the primary bedding throughout near-fully pyritic Top Plessey samples (Fig. 3c). In other samples where cleats are evident but much less common such as Durham Low Main samples, cleats form perpendicular to bedding-parallel cleats, and also form along planes of weakness, such as at the edge of kaolinite minerals (Fig. 3d).

Samples taken from the Durham Low Main and Top Plessey seams often contain higher amounts of cleat-filling pyrite, while Plessey, Top Busty and Bottom Busty seams contain more disseminated pyrite phases. Disseminated framboidal and cubic pyrites are typically inclusion-free and may be associated with clay minerals such as kaolinite (Fig. 3b). Cleat-filling pyrite cross-cuts disseminated pyrite, or fractures run along the outer edge of the disseminated pyrite, exploiting the plane of weakness (Fig. 3d). Cleat-filling pyrite is more commonly associated with abundant hexagonal, booklet-like kaolinite (Fig. 3c) and needle-like gypsum (Fig. 4a), and contains minor inclusions of baryte (up to 5 μm; Fig. 4b), sphalerite (< 2 μm; Fig. 4c) and galena (< 2 μm; Fig. 4d).

4.2. Whole rock geochemistry

General coal properties from sampled seams as a whole seam representation are shown in Table 1. Previous work on Northumberland coal has considered a total S content of above 1.3% as high, as this is the cut-off value for the S content of coals acceptable for local power generation (Turner and Richardson, 2004). Shotton site samples show anomalously high S contents, up to 30.1% in Top Plessey seam pyritic coal samples (Table 2) and an overall average of 12%. Top Plessey samples also show high Fe content (up to 25.5%). High S and Fe in these samples reflect the high (often cleat-filling) pyrite content. Other non-pyritic seam samples show S content of 0.3% (Top Busty) to 5.3%
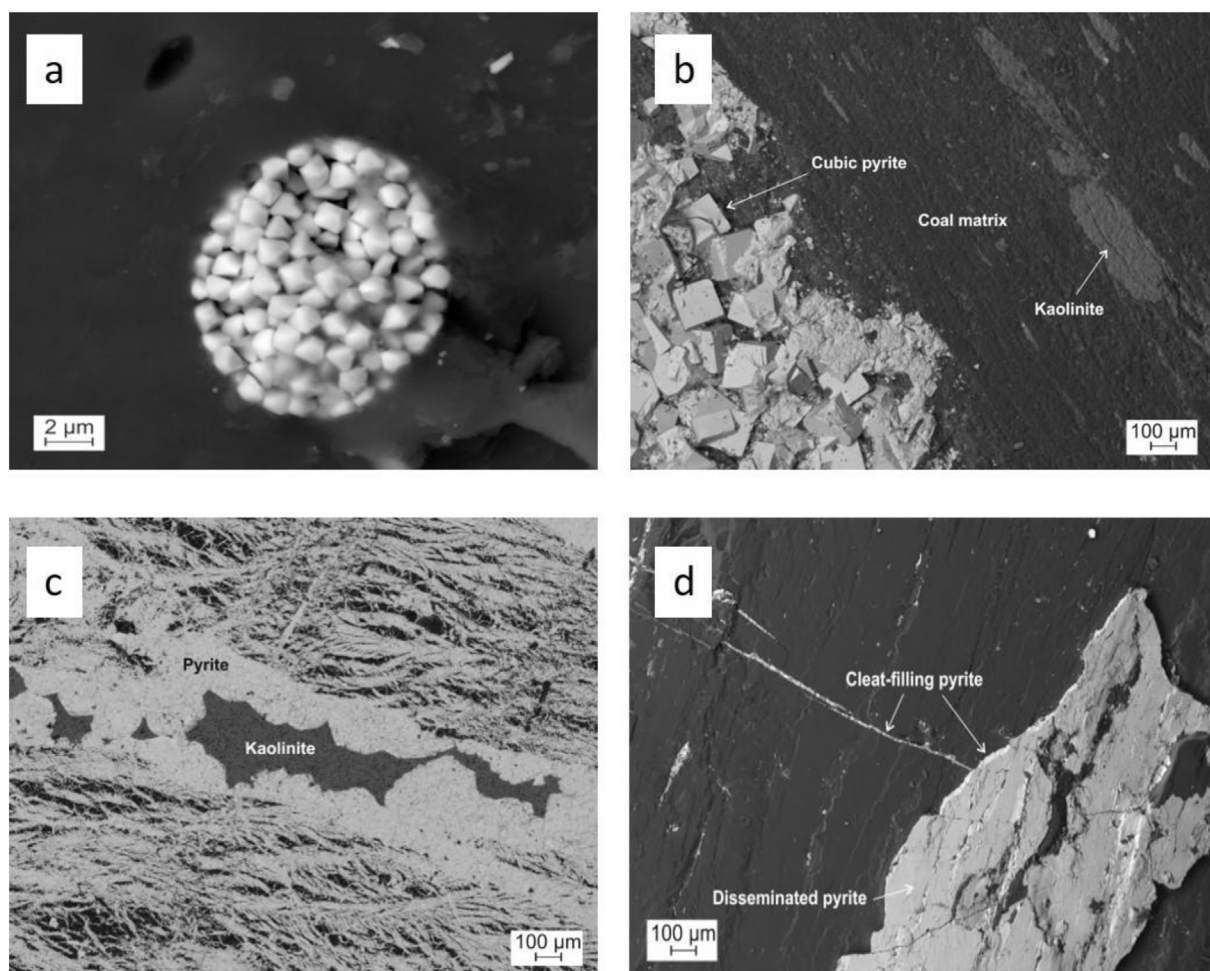

Fig. 3. Microscopic (SEM) backscattered electron images of the main pyrite phases in Northumberland coals: (a) framboidal disseminated pyrite in Durham Low Main coal seam sample, (b) cubic disseminated pyrite and kaolinite in Plessey coal seam sample, (c) cleat-filling pyrite, with pyrite concentrating in an intricate network of fractures, veins and veinlets; kaolinite also present (Top Plessey seam), and (d) cleat-filling pyrite and disseminated pyrite (Durham Low Main seam). Cleat-filling pyrite also forms alongside the edge of the disseminated pyrite at plane of weakness.
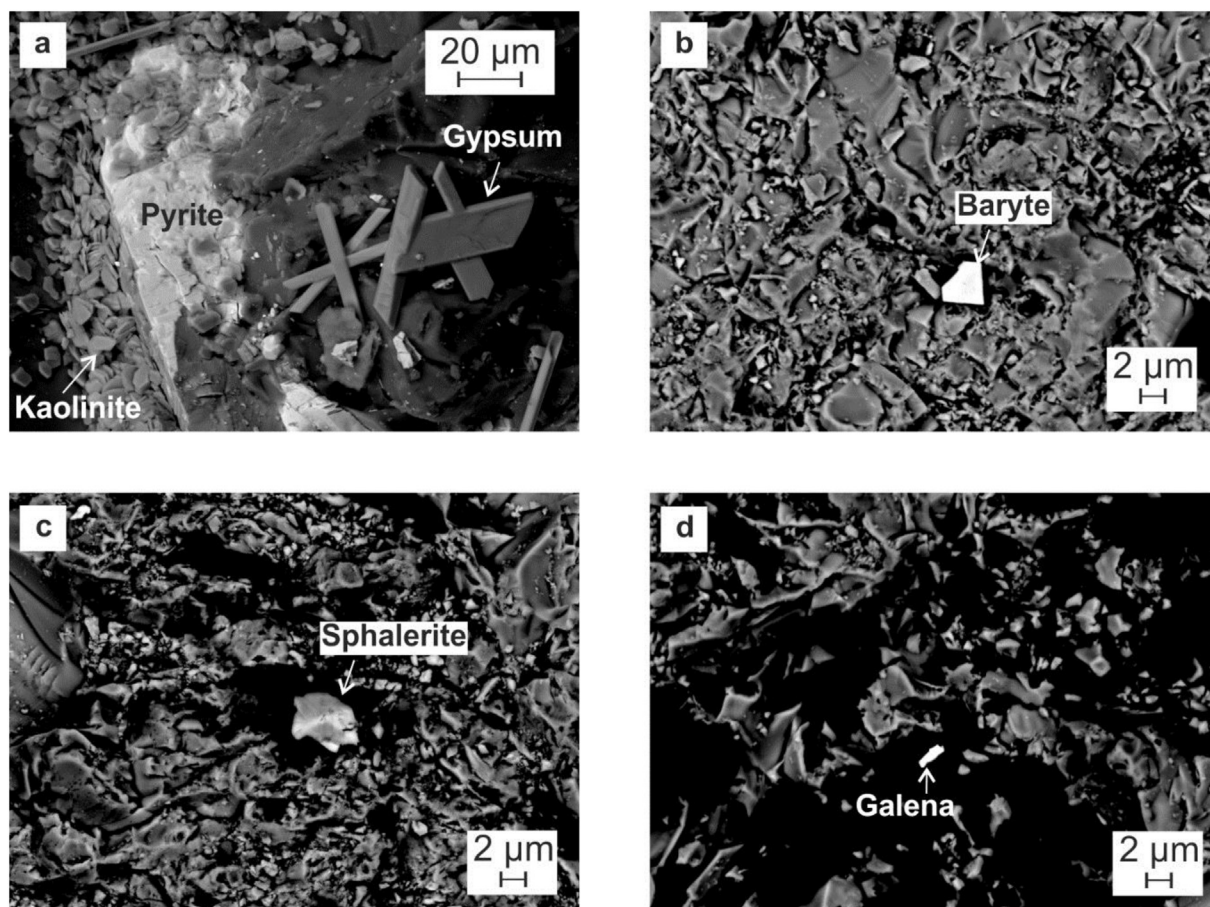
Fig. 4. Microscopic (SEM) backscattered electron images of minor mineral phases associated with cleat-filling pyrite: (a) kaolinite and gypsum, (b) baryte, (c) sphalerite, and (d) galena.

(Durham Low Main). By comparison, other sampled Northumberland coals show an average total S content of 1.1%. The Top Busty seam contains the highest TOC (66.5%), while Top Plessey samples generally contain the lowest TOC (22.1% to 31.1%, with one exception of 63.9%, Table 2). The average TOC of other sampled Northumberland coals (56.5%) is higher than the average TOC of Shotton coals (44.1%).

The average Se content of Shotton coals is 16.5 ppm, and the overall average for sampled Northumberland coals is 12.1 ppm. Pyrite-rich coals show higher Se than non-pyritic coals (Table 2). Top Plessey seam samples contain anomalously high Se content, up to 61.9 ppm and with an average seam Se content of 26.4 ppm. Though no other Northumberland coals show Se contents this high, the Durham Low Main

Table 2
Whole coal concentrations (on an as-determined basis) for samples from the Shotton site and nearby coal exposures in Northumberland (pyritic and non-pyritic coals).

Sample description	Fe (%)	S (%)	Se (ppm)	TOC (%)	$\delta^{34}S$ (‰)
Shotton Opencast Surface Mine coal seams					
Durham Low Main (framb, cubic, minor cl py, < 10% sample area)	3.3	5.3	5.9	57.5	9.0
Northumberland Low Main (generally non-pyritic, < 10%)	0.1	0.4	1.0	61.5	–
Top Plessey (Top Leaf) (generally non-pyritic, < 10%)	0.02	0.4	0.6	64.7	–
Top Plessey (Top Leaf) (generally non-pyritic, < 10%)	0.02	0.2	0.5	62.7	–
Top Plessey (Top Leaf) (cl py, > 40% sample area)	17.4	23.4	44.0	31.1	8.3
Top Plessey (Top Leaf) (cl py, > 40% sample area)	19.9	30.1	61.9	22.6	–
Top Plessey (Bottom Leaf) (cl py, > 40% sample area)	21.0	23.1	26.2	30.4	–
Top Plessey (Bottom Leaf) (cl py, > 40% sample area)	17.9	28.8	42.2	22.3	11.7
Top Plessey (Bottom Leaf) (cl py, > 40% sample area)	25.5	27.5	9.6	22.1	–
Plessey (generally non-pyritic, minor cubic, < 10%)	0.07	2.3	1.6	52.9	− 20.6
Top Busty (generally non-pyritic, < 10%)	0.02	0.3	0.4	66.5	–
Bottom Busty (generally non-pyritic, minor cubic, < 10%)	3.1	2.6	4.6	53.9	–
Other Northumberland sample sites					
Ellington (av. 16 seams; data from Bragg et al., 1998) (pyritic)	14.5	1.8	3.4	54.8	–
Whitley Bay (non-pyritic)	0.04	0.4	0.5	62.4	–
Potland Burn (non-pyritic)	0.02	0.4	1.0	62.1	–
Lynemouth pyritic coal (pyritic)	10.1	2.0	1.2	46.0	–
Lynemouth pyritic coal (non-pyritic)	0.5	0.8	0.8	57.2	–

py = pyrite; framb = framboidal, cl = cleat-filling; (−) = not analysed.
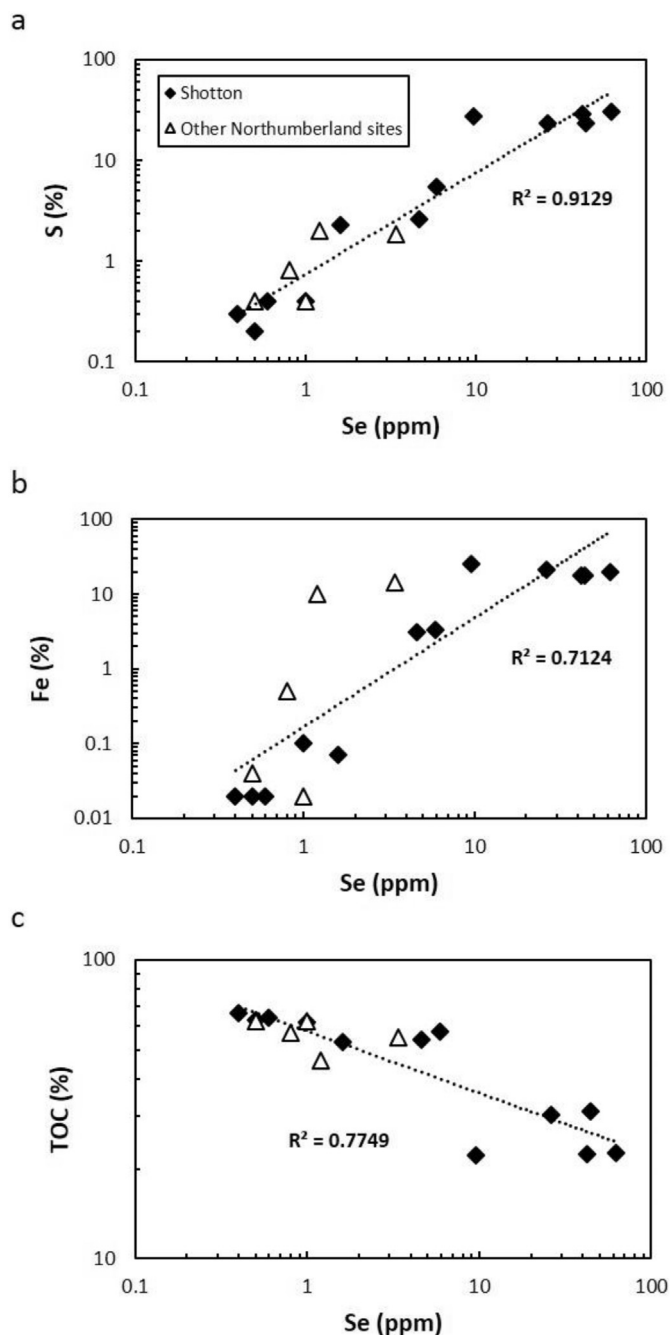
Fig. 5. Cross-plots of Se vs. (a) S, (b) Fe, and (c) TOC. Trend lines and correlation value (R^2) also shown.

Table 3
Iron (Fe) and selenium (Se) concentrations in pyrite from the Shotton site and other local coal exposures in Northumberland.

Sample description	Fe (%)	Se (ppm)
Shotton Opencast Surface Mine coal seams		
Durham Low Main	19.0	32.5
Northumberland Low Main	24.8	20.8
Top Plessey	24.6	39.4
Top Plessey	29.2	126.8
Plessey	33.9	8.8
Top Busty	24.9	3.1
Bottom Busty	20.0	2.5
Bottom Busty (coal matrix)	2.3	6.4
Other Northumberland sample sites		
Lynemouth coal, Morpeth	31.4	8.2
Lynemouth coal, Morpeth	25.4	6.4
Lynemouth coal, Morpeth	37.9	9.7
Lynemouth coal, Morpeth	5.0	13.0

126.8 ppm), generally increasing upward through the sequence from Bottom Busty (Lower Coal Measures) to Durham Low Main (Middle Coal Measures) (Table 3). Top Plessey pyrite samples show the highest average Se for pyrite (39.4 and 126.8 ppm), while Bottom Busty pyrite has the lowest average Se content (2.5 ppm). Northumberland Low Main pyrite contains an average Se content of 20.8 ppm. Pyrite from nearby Lynemouth pyritic coals show average Se concentrations from 6.4 ppm up to 13 ppm, with a similar range of concentrations to that of Bottom Busty (2.5 to 6.4 ppm), Top Busty (3.1 ppm) and Plessey (8.8 ppm) from the Shotton site. Two types of pyrite can be identified in SEM imagery (Fig. 3) and based on laser ablation maps (Fig. 6): disseminated phases in all seam samples, and cross-cutting cleat-filling pyrite predominantly found within Top Plessey seam samples. Laser ablation maps show that Se commonly comprises the pyrite crystal structure (Plessey, Top Busty and Bottom Busty pyrites; Fig. 6). There are higher Se concentrations in cleat-filling pyrite (up to 250 ppm in Top Plessey pyrite; Fig. 6) compared to disseminated pyrite (generally 10–20 ppm in Plessey, Top Busty and Bottom Busty pyrites; Fig. 6). In some instances, the coal matrix also shows enriched Se content (up to 10 ppm in the Plessey coal matrix; Fig. 6) compared to the averages for UK and world coals.

4.4. Sulphur isotope compositions

Four pyrite samples (extracted from Durham Low Main, Top Plessey (Top Leaf), Top Plessey (Bottom Leaf) and Plessey seams) were measured for their S isotopic compositions. Plessey samples were extracted as disseminated phases, while Durham Low Main and Top Plessey samples were extracted from cleats. The $\delta^{32}S$ compositional range is −20.6‰ to +11.7‰. The disseminated Plessey pyrite sample shows a $\delta^{32}S$–enriched (isotopically light) composition of −20.6‰, while cleat-filling Durham Low Main, Top Plessey (Top Leaf) and Top Plessey (Bottom Leaf) pyrites show $\delta^{34}S$–enriched (isotopically heavy) compositions (+9.0‰, +8.3‰ and +11.7‰ respectively).

5. Discussion

5.1. Selenium-hosting pyrite formation

Pyrite is the dominant host of Se in Northumberland coal samples (Table 2 and Fig. 6), though organic matter also contains slightly elevated Se content (Fig. 6). Though pyrite is the main Se host, there is evidence for elevated Se in some matrix samples (up to 10 ppm in Bottom Busty) compared to the averages of UK and world coals, indicating some organic-bound Se. However, the lack of positive correlation between Se and TOC indicates a negligible role played by organic matter in Se enrichment in Northumberland coals. The different forms
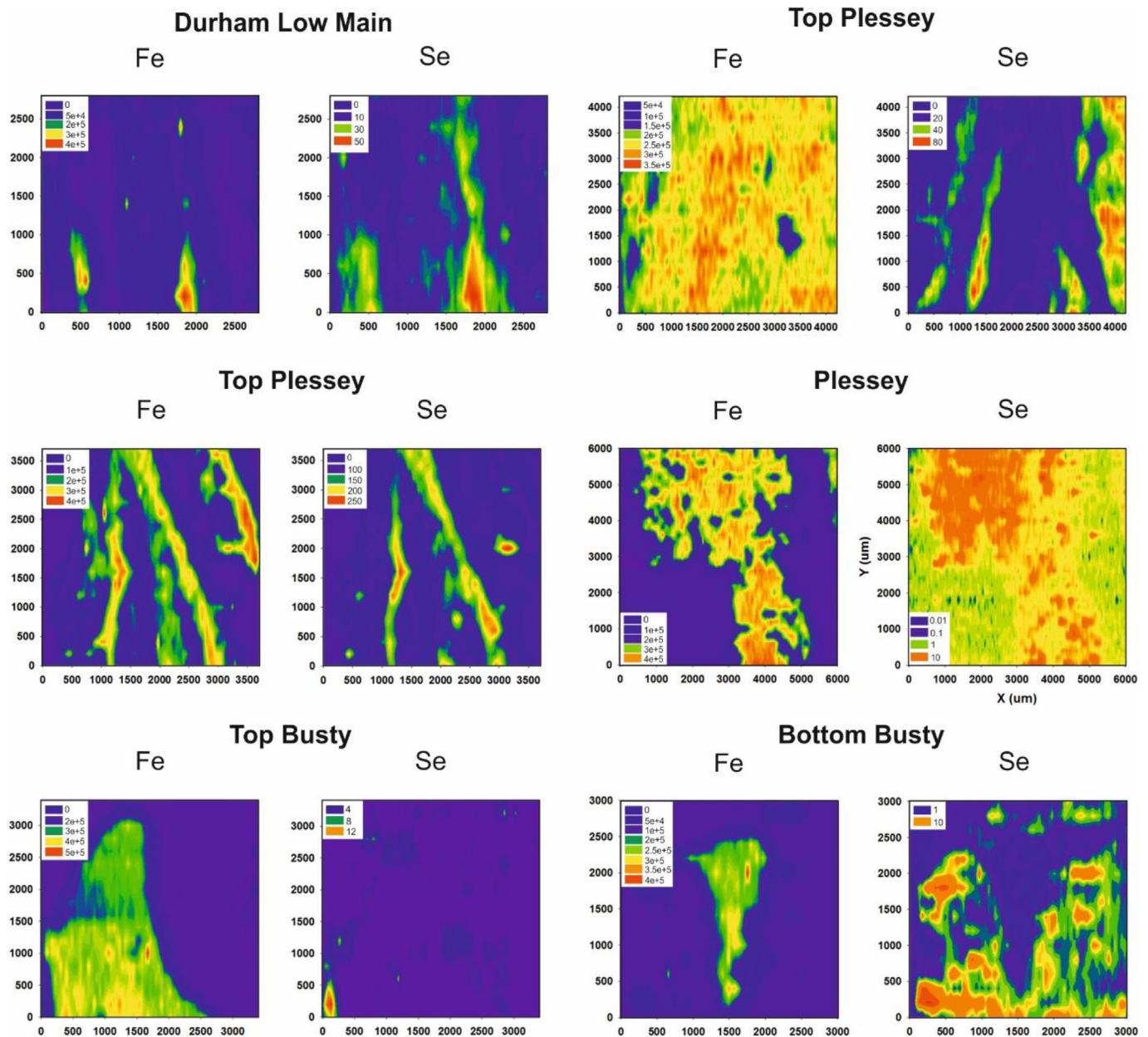
sample (5.9 ppm) and Bottom Busty sample (4.6 ppm) are higher than the mean Se values for the common UK and world coals. Ellington samples (Bragg et al., 1998) also show higher Se content (3.4 ppm) than the averages for UK and world coals. Northumberland coals show a strong correlation between Se and S ($r^2 = 0.91$; Fig. 5a), and there is a relatively strong correlation between Se and Fe ($r^2 = 0.71$; Fig. 5b). Conversely, Se and TOC show a slight inverse relationship ($r^2 = 0.77$; Fig. 5c).

4.3. Pyrite chemistry

The Se content of the analysed pyrite samples is variable (3.1 to

Fig. 6. Laser ablation maps and concentrations (ppm) of pyrite crystals from selected Shotton site coal seams. Iron (Fe) maps are shown to indicate the pyrite phase. Note cleat-filling pyrites (Durham Low Main and Top Plessey) show elevated Se content (up to 250 ppm) compared to disseminated pyrite phases (Plessey, Top Busty and Bottom Busty, up to 12 ppm). In one instance, the coal matrix shows higher Se content (up to 10 ppm) than in the disseminated pyrite (Bottom Busty).

of pyrite and occurrence of individual framboidal pyrites indicates multiple stages of pyrite formation (Kostova et al., 1996; Dai et al., 2003; Dai et al., 2015b). Petrographic evidence shows that there were multiple stages of syngenetic or early diagenetic pyrite mineralisation, with later cleat-filling pyrite cross-cutting earlier formed framboidal and cubic pyrite. Petrographic observations (Fig. 3), laser ablation maps (Fig. 6) and the wide range of isotopic compositions indicate at least two generations of pyrite formation: (1) syngenetic and epigenetic (disseminated framboidal and cubic) pyrite, and (2) later epigenetic, cross-cutting cleat-filling pyrite, similar to the multiple pyrite generations of Se-rich Ayrshire Carboniferous coals (Bullock et al., 2018b).

UK Coal Measures cleat formation is primarily controlled by tectonism following uplift and release of overburden pressure (Rippon, 1996). Variscan tectonics of the late Carboniferous and early Permian deformed the Coal Measures of Northumberland into gentle folds and extensive faulting (Arthurton et al., 1989; Rippon, 1998; Stone et al.,

2010). Thus, pyrite-coating cleat surfaces post-dates cleat formation and coalification and are therefore thought to be post-depositional epigenetic pyrite in Northumberland samples (Turner and Richardson, 2004). Cleats have been observed to form both parallel and perpendicular to bedding, which may suggest cleat formation occurred in multiple stages. This observation is similar to the cleat development observed in Westphalian A–C aged sediments in the South Wales coalfield (Gayer et al., 1996). Here, the authors noted that cleats pre-date fold and thrust development, and are observed in lignites, both indicating relatively early cleat development. The authors also identified butt cleats forming at right angles to face cleats, attributed to exhumation. Both observations indicate an early onset, preceding further episodes of cleat formation, which is also suggested here for Northumberland coal cleat development. Similar joint pattern observations were made by also Price (1959, 1966) at the Whin Sill and adjacent sediments in nearby Upper Teesdale (Spears, 1961), approximately 30 miles from the

Shotton site.

Isotopically lighter compositions, resulting from pyrite formation by microbial sulphate reduction (Parnell et al., 2013), coincide with disseminated pyrite, while isotopically heavier compositions represent cleat-filling pyrite, associated with cleats formed later (possibly during Variscan activity). The δ^{32}S–enriched isotope composition in Plessey disseminated pyrite is consistent with bacteriogenic (microbially-formed) pyrite, and whole rock Plessey contains 1.6 ppm Se, similar to world coal Se compositions. This suggests that microbially-formed disseminated pyrite may slightly elevate Se content, but not significantly compared to world mean values.

The widespread occurrence of kaolinite with cleat-filling pyrite suggests that later pyrite within cleats may have formed from acidic waters at shallow depths (< 2 km) and low temperatures ($< 100\,°C$) (Dunoyer de Segonzac, 1970; Ruiz Cruz and Reyes, 1998; Tucker, 2012), following cleat-forming brittle deformation. In Shotton site seam samples, Se is enriched in cleat-filling pyrite (up to 250 ppm in Top Plessey) compared to earlier formed disseminated pyrite (10–20 ppm; Durham Low Main, Plessey and Top Busty), showing that later-formed pyrite is predominantly responsible for high Se. This is particularly true of Top Plessey samples, which contain areas of abundant cleat-filling pyrite. This higher pyrite abundance also accounts for the highest Se concentrations identified in this study. Cleats can provide channels for fluid flow, and a locus for epigenetic and hydrothermal pyrite precipitation and associated higher Se concentrations (Hatch et al., 1976; Bullock et al., 2018b). Cleat-filling and later formed pyrite has been previously shown to contain elevated trace element content in UK and worldwide coals (Finkelman, 1980; Spears and Amin, 1981; Spears and Caswell, 1986; White et al., 1989; Spears and Zheng, 1999; Goldhaber et al., 2000; Ding et al., 2001; Diehl et al., 2012; Yudovich and Ketris, 2005; Spears and Tewalt, 2009; Bullock et al., 2018a, 2018b). The noticeably high Se at the Shotton site in Middle Coal Measures seams compared to regional and British coals suggests a localised enrichment mechanism in the Shotton site area (see section 5.2).

5.2. Selenium source

Northumberland coals show elevated Se contents compared to other British coals, including anomalously high Se pyritic coals of Ayrshire (Bullock et al., 2018b), Argyllshire, Fife-Stirling, Cumberland, Nottinghamshire, North Wales and Staffordshire (Bullock et al., 2018a). There are two probable options for the source of high Se in the Northumberland coals that have been previously postulated: (1) Ore fluids from the Lower Carboniferous North Pennine Orefield to the south of the region, and/or (2) a seawater distribution influence with periodic inundation by the sea into low-lying deltaic planes. Spears (2015, 2017) discusses these possible source origins in detail for UK coals across the northern Pennines and Northumberland. Goldschmidt (1943) first suggested a link to ores in the Lower Carboniferous North Pennine Orefield, with the proposal of detwatering of adjacent basins as a source of hydrothermal fluids, which was later considered by Dunham (1988) and discussed as a possibility by Turner and Richardson (2004). Variscan compressional tectonics may have expulsed hot, metalliferous fluids from depth, with movement northwards and upwards through the Coal Measures towards the basin margin and possibly along basin margin faults (Mills and Holliday, 1998; Turner and Richardson, 2004). Turner and Richardson (2004) present S isotope data that may support a link to the North Pennine Orefield, but this is only achievable if a measurement of $+32.8‰$ is excluded. This high δ^{34}S value exceeds the value of $+18‰$ for Lower Carboniferous seawater sulphate, suggesting that the system was open to the addition of δ^{34}-enriched sulphur (McKay and Longstaffe, 2003; Turner and Richardson, 2004), which in turn argues for a possible Lower Carboniferous marine sulphate source for some of the sulphur (Turner and Richardson, 2004).

The Northumberland region contains coals of high thermal maturity, evident by high vitrinite reflectance values of 1.3% to 1.6% (Burnett, 1987; Armstroff, 2004). This high thermal maturity may relate to the high Se content in coals. Igneous intrusions can provide the necessary heat to the coal strata to increase vitrinite reflectance and may also result in Se-carrying hydrothermal fluids percolating through coals, precipitating as later cleat-filling pyrite. This has been previously suggested for Carboniferous coals in Ayrshire (Bullock et al., 2018b) and Jurassic coals in Brora, Sutherland (Bullock et al., 2017). The proximity of the Northumberland coalfield to the Weardale granite in North East England, and the associated Variscan (late Carboniferous to early Permian) mineralisation and deformation (which produced a series of faults through the coal strata, forming cleat systems), may have provided both a source and a flow pathway for hot Se-rich fluids and increased maturity to Northumberland coals (see also Turner and Richardson, 2004).

Cann and Banks (2001) identified four possible hydrothermal fluids, two from the evaporation of seawater, with little significant contribution from dewatering of the adjacent basins. The main phase of ore generation was considered took place during the Late Permian, permitting saline waters to penetrate deep into the basement. Bouch et al. (2006) identified an early phase of alteration responsible for pervasive dolomitisation and ankeritisation, in the presence of a high salinity brine. These compositions are consistent with fluids that would have been expelled from progressively maturing basinal shales, potentially from the Late Carboniferous into the Early Permian. Spears (2015, 2017) uses this evidence to conclude that a direct link between high trace element concentrations in the coals and the origin of the ore fluids on the adjacent blocks is unlikely. Spears (2015) also considered the timing of the cleat infill, which consists of (a) sulphides, (b) silicates and (c) carbonates. This is a common paragenetic sequence and has been linked to diagenetic sequences in associated clastic sediments, which takes place during normal burial diagenesis. It is therefore concluded that the cleat minerals formed in response to pore fluid evolution and movement during burial diagenesis. High Se Shotton coals compared to the rest of the Northumberland sample suite suggests a possible localised means of trace element enrichment, particularly in the Top Plessey seam of the Middle Coal Measures. The Shotton site is faulted, and contains dykes, which may further affect the Se content by introducing more fractures and trace element-rich fluids, particularly evident by high Se pyrite in cleats and fractures of sampled coals, though this is only speculated here.

5.3. Regional comparisons

High Se coals from Shotton (maximum 61.9 ppm) are comparatively higher than other anomalous Se coals worldwide, except for some northern Appalachian coals (Table 4, Fig. 7) and Chinese coals. Anomalous seleniferous coals and stone coals have been extensively studied across the carbonate platform of China in areas such as Guauangxi, Yunnan and Xinjiang (Cheng, 1980; Mao et al., 1988, 1990; Song, 1989; Su et al., 1990; Zheng et al., 1992, 1999; Finkelman et al., 2002; He et al., 2002; Lei, 2012; Zhu et al., 2012; Dai et al., 2012, 2015a,b, 2017, 2018a,b), unique in world coals, and are thus excluded from these comparisons (with the exception of some organic or Pb-sulphide affiliated Se occurrences; see Section 5.4). Elsewhere, extensively studied U.S. coals show Se content of 75 ppm (northern Appalachian coals and Iowa; Coleman et al., 1993). Here, a lack of correlation between Se and either organic or pyritic sulphur led to the suggestion that there may have been multiple sources of Se, including detrital particles, plant matter, volcanic ash, surface water and groundwater, and epigenetic mineralisation (Coleman et al., 1993). High S bituminous coals of southern Illinois contain up to 46 ppm (Carter et al., 1975). However, this high value is based on an ash basis rather than a whole rock basis, similar to previously identified high Se Texas Paleogene lignites (up to 77 ppm on the ash basis; Clark et al., 1980). Kentucky coal samples contain pyrite-filled veins with an average of 200 ppm Se (Diehl et al., 2012), which is similar to

Table 4
Maximum Se concentrations (whole coal) for the Shotton site and other notable Se-bearing coals reported worldwide.

Locality	Sample type	Se (ppm)	Se mode of occurrence	Whole coal measurement method	Source
Northern Appalachia, USA	Unknown	75	Mixed occurrences	INAA	Coleman et al., 1993; Stillings, 2017
Shotton, Northumberland, UK	Seam picks	62	Sulphide-dominated	ICP-AES	This study
Alaska, USA	Unknown	43	Unknown	ICP-AES	Bragg et al., 1998
Guilding and Heshan, China	Chanel	32	Organic affiliation	ICP-MS	Liu et al., 2015
Kalishur, Iran	Channel	32	Organic affiliation	INAA	Pazand, 2015
Muğla, Turkey	Channel	26	Unknown	ICP_AES	Bragg et al., 1998
Sunchon, DPR Korea	Unknown	22	Unknown	ICP_AES	Bragg et al., 1998
Gangwon-Do, Republic of Korea	R-O-M	21	Unknown	ICP_AES	Bragg et al., 1998
Mississippi, USA	Feed stocks	21	Organic affiliation	ICP-AES	Warwick et al., 1995
Wyoming, USA	Unknown	16	Organic affiliation	ICP-AES	Dreher and Finkelman, 1992; Stricker and Ellis, 1999
Svalbard, Norway	Channel	15	Unknown	ICP-AES	Bragg et al., 1998
Ellington, Northumberland, UK	Unknown	15	Sulphide-dominated	ICP-AES	Bragg et al., 1998
Ayrshire, UK	Seam picks	15	Sulphide-dominated	ICP-AES	Bullock et al., 2018b
Ioannina, Greece	Cores	14	Leaching of evaporites	INAA	Gentzis et al., 1997; Yudovich and Ketris, 2006
Kabul, Afghanistan	Channel	12	Sulphide-dominated	ICP-AES	Bragg et al., 1998
Shandong, China	Bulk	10	Organic affiliation	ICP-AES	Liu et al., 2006
Donetsk, Ukraine	Seam picks	10	Sulphide-dominated	ICP-AES	Yudovich and Ketris, 2006; Kolker et al., 2009
Elk River Valley, Canada	Pit wall picks	9	Mixed occurrences	ICP-OES	Lussier et al., 2003
Sokolov, Czech Republic	Unknown	6	Organic affiliation	Unknown	Pešek et al., 2005
Great Greta, Australia	Seam	4	Organic affiliation	HG-AFS	Riley et al., 2007
Pennsylvania, USA	Unknown	3	Organic affiliation	EMP	Finkelman, 1980
Alabama, USA	Unknown	3	Organic affiliation	Multi-analytical	Fiene et al., 1979
Lake Baikal, Russia	Unknown	0.9	Organic affiliation	Unknown	Troshin et al., 2001

Sample type: R-O-M = Run-of-mine Method of measurement: ICP-AES = inductively coupled atomic emission spectrometry; ICP-MS = inductively coupled plasma mass spectrometry; ICP-OES = inductively coupled optical emission spectrometry; EMP = electron microprobe; HG-AFS = hydride generation atomic fluorescence spectrometry; INAA = instrumental neutron activation analysis.

maximum pyrite concentrations at Shotton (~250 ppm in Top Plessey coal seam sample; average of 127 ppm across pyrite in sample; Fig. 6). Mississippi lignites contain up to 20.3 ppm Se on a whole coal basis (Warwick et al., 1995), and Paleogene lignites of Alaska contain up to 43 ppm Se whole coal (Bragg et al., 1998).

In other locations worldwide, Iranian coals have been studied for their high Se content, up to 31.5 ppm, influenced by metamorphism, tectonic conditions and oxygenated waters (Pazand, 2015). Ukrainian high S bituminous coals (S = 2.9%) have been noted to contain anomalous Se, with a maximum of 9.8 ppm (Yudovich and Ketris, 2006), while the Pleistocene Megalopolis deposit (Greece) contains up

to 11.1 ppm Se (Foscolos et al., 1989). Neogene Ioannina high S and high ash lignites (Greece) also contain enhanced Se content to 13.9 ppm Se (Yudovich and Ketris, 2006). High Se in Ioannian lignites is attributed to leaching from gypsum and/or anhydrite beds in the area (Gentzis et al., 1997). Other notably high Se coals worldwide from the world coal database (Bragg et al., 1998) include Pliocene coals of Afghanistan (up to 12 ppm), Permian anthracitic coals of DPR Korea (22 ppm), Republic of Korea Carboniferous to Early Permian coals (21 ppm), Tertiary coals of Norway (15 ppm) and Tertiary coals of Turkey (26 ppm) (Bragg et al., 1998) (Table 4, Fig. 7).

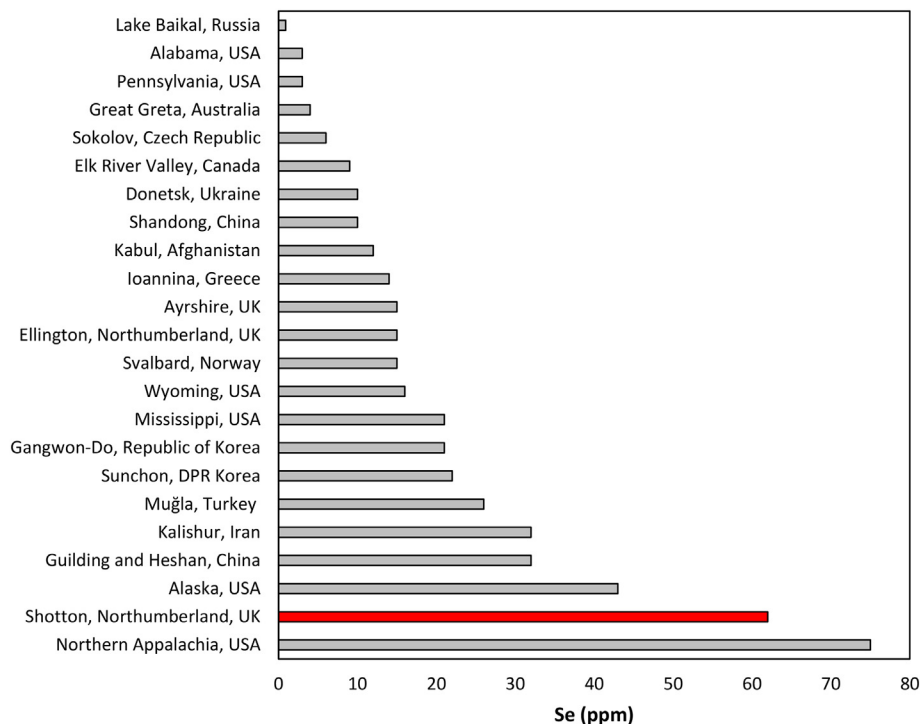In the UK, Se content averages approximately 1.3–2.1 ppm (Spears

Fig. 7. Bar plot of notably high (maximum) Se in worldwide coals. Shotton site coals (red bar) show maximum concentrations higher than or comparable to other notable maximum Se world coals. See Table 4 for references. (For interpretation of the references to colour in this figure legend, the reader is referred to the web version of this article.)
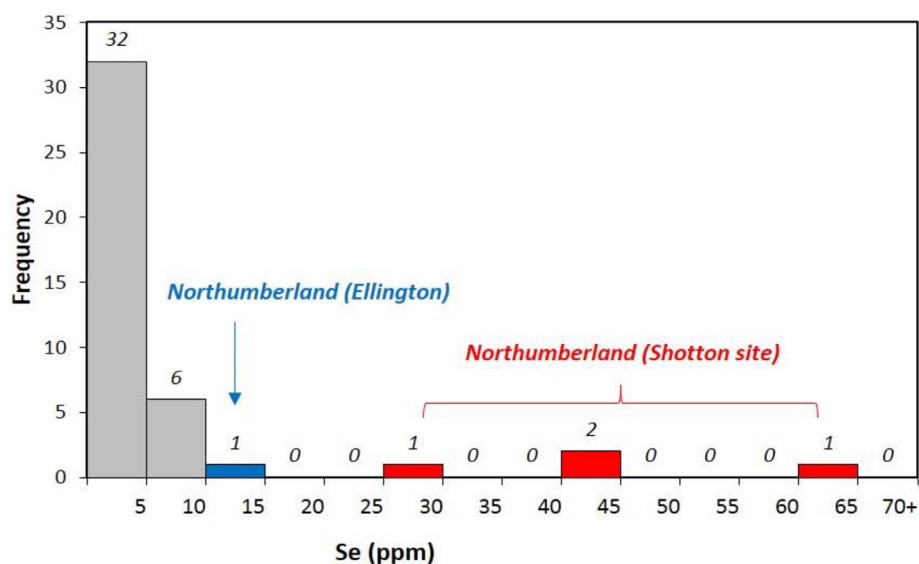
Fig. 8. Histogram of measured Se in British coals (Bullock et al., 2018a). Most British coals contain Se of < 10 ppm, emphasising the anomalous nature of Ellington (blue bar, Bragg et al., 1998) and Shotton site coals (red bars) of Northumberland. (For interpretation of the references to colour in this figure legend, the reader is referred to the web version of this article.)

and Zheng, 1999; Bullock et al., 2018a), with notably high Se in Ayrshire (15 ppm; Bullock et al., 2018b) and Ellington, Northumberland (Bragg et al., 1998). Samples of coals with no visible pyrite from nearby Whitley Bay and Potland Burn contain Se content of 0.5 ppm and 1.0 ppm respectively (Table 2). However, samples from Ellington are generally higher than the averages of UK and world coals, containing an average of 3.4 ppm and a maximum of 15 ppm (Bragg et al., 1998). Ellington and Shotton site Se concentrations are anomalous compared to other UK coal samples (Figs. 7–8), and the high Se at Ellington suggests that high Se is evident on a regional scale in Northumberland. Other UK coals generally contain < 4 ppm Se, with some anomalous localities showing 4–6 ppm Se (Argyllshire, Fife-Stirling, Nottinghamshire, North Wales and North Staffordshire Coalfields; Bullock et al., 2018a). These anomalous coals are also typically high in S and pyrite content. The histogram in Fig. 8 emphasises the unusually high Se content of Shotton site coals compared to other UK coals. Selenium concentrations in pyrite from UK coals (measured by different mineral chemistry methods) include 78 ppm (Parkgate; Spears, 2015), 97 ppm (East Midlands; White et al., 1989), 38 ppm (Harworth; Spears et al., 1999) and 27 ppm (Eggborough; Spears and Booth, 2002). These results compare well to the values obtained for pyrites in this study (range of Se compositions from 2.5 ppm to 126.8 ppm, average of 30 ppm), and further emphasise the role of pyrite in Se enrichment in UK coals.

5.4. Modes of occurrence comparisons

The dominant forms of Se in coals are inorganic (hosted within sulphides, such as pyrite as documented in this study) and organic affinities. Comparing the maximum Se content of Northumberland coals (in pyritic form) to notable coals with organic Se as the dominant mode of occurrence, the coals of Northumberland are anomalously higher (Table 4). High Se of up to 32 ppm has been identified in coals of Guilding and Heshan in China (Liu et al., 2006), and in Kalishur, Iran (Pazand, 2015). The low-ash subbituminous coals of the Powder River Basin (Wyoming, USA) are considered to contain Se comprising up to 60% organic affinities (Dreher and Finkelman, 1992), and show concentrations of up to 16 ppm (Stricker and Ellis, 1999). The Shanxi Formation, Yanzhou Coalfield, China, contains organic Se of up to 10 ppm (Liu et al., 2006), and Czech coals in the Sokolov Basin contain organic Se of up to 6 ppm (Pešek et al., 2005). Elsewhere, organic associated Se is typically low (e.g. 0.9 ppm at Lake Baikal, Russia, Troshin et al., 2001; up to 4 ppm in Great Greta, Australia, Riley et al., 2007; up to 3 ppm in the Upper Freeport coal, Finkelman, 1980; up to 3 ppm at Blue Creek, Alabama, Fiene et al., 1979).

Other micro-mineralogical sulphide host Se phases in coal include trace Pb-bearing minerals, such as clausthalite (PbSe), galena and selenio-galena (Finkelman et al., 1979; Finkelman, 1980; Hower and Robertson, 2003; Dai et al., 2006, 2008; Li and Zhao, 2007). Examples of Se-hosting trace phases include ferroselite ($FeSe_2$), krutaite ($CuSe_2$), and eskebornite ($CuFeSe_2$) (Dai et al., 2015a). These modes of Se enrichment have yielded whole coal contents of up to 18 ppm in Eastern Kentucky and 13 ppm in Western Kentucky (Bragg et al., 1998; Hower and Robertson, 2003), and up to 16 ppm in the No. 6 Coal in the Junger Coalfield of the Ordos Basin, China (Dai et al., 2006, 2008; Li and Zhao, 2007). The overall abundance of high-Se cleat-filling pyrite identified in the Top Plessey seam samples from Northumberland contributes to the highest Se values recorded in this study, anomalous on a regional and worldwide scale.

5.5. Considerations

At the time of writing, the Shotton site is estimated to contain approximately 800,000 t of coal that could be extracted (Gary Morgan (Banks Group), perso. comms., 2018). Assuming an average Se site content of 17 ppm, this suggests that there could be 13,600 kg of Se in the Shotton coal reserve. At present, despite the high whole rock and pyrite concentrations, Shotton coals cannot be considered economic for Se (current suggested estimated cut off grades in coal = 500–800 ppm, based on cut-off grade of stone-like coal; Dai et al., 2018b; Lin et al., 2018). This is due to the current limitations and inadequate means of Se extraction. However, with increasing demand for Se and improved means of extraction, existing sites where sources of Se are already exposed, mined and (at least partially) processed may be important. Recent advances in sorbent technologies have led to the improved retention, capture and recovery potential of Se (Diaz-Somoano and Martinez-Tarazona, 2004; Ghosh-Dastidar et al., 1996; López-Antón et al., 2007; Tian et al., 2014; Lin et al., 2018), and Se recovery from coal as a by-product may help to address the critical materials demand, and offset emission control costs of coal and gasification plants (Lin et al., 2018). Identification of specific seams of high Se content, and the mechanisms of enrichment associated with these seams, make it easier to pinpoint the potentially economically viable Se hosts, both here and in similar sites of multi-generational pyrite-hosted coals worldwide. Pyrite has already been identified as a potentially significant Se source (Keith et al., 2017), so the high pyrite content of exposed Top Plessey seams could make a suitable Se resource. Operations at the Shotton site are set to close by 2021, and high Se coals should be managed to avoid liberation during any further excavation and restoration. Remaining coal

spoil deemed too high in S content for power generation or domestic use may form an important Se resource for alloys, photovoltaic products and nanotechnologies. The role of enrichment indicates that similar coal sites containing early disseminated and late cleat-filling pyrite may also contain high Se coal seams and warrant further attention as demand continues to rise.

6. Conclusions

The Carboniferous Coal Measures coals of Northumberland contain anomalous concentrations of Se, significantly enriched compared to the average of UK and world coals. Pyrite is the main mode of occurrence for Se in the analysed samples. Enrichment across sample sites in Northumberland suggests a regional influence on concentrations. Coals are highly pyritic, with evidence for multiple stages of pyrite generation (early disseminated and later cleat-filling pyrite). While microbially-formed (earlier) pyrite can enrich Se above UK and world mean compositions, the later-formed (later diagenetic and hydrothermal), more spatially abundant cleat-filling pyrite shows significant enrichment of Se up to 250 ppm in sampled seams. Trace element enrichment in this region is likely influenced by seawater distribution, and dykes and associated deformation may also locally affect Se content of coals at the Shotton Surface Mine. Increasing demands for E tech elements, future developments in pyrite extraction and identification as a potential source of trace metals means that sites such as Shotton and coal mining regions such as Northumberland and others worldwide may host important Se concentrations and should be considered before operations cease production.

Acknowledgments

References

Abzalov, M.Z., 2012. Sandstone-hosted uranium deposits amenable for exploitation by in situ leaching technologies. Appl. Earth Sci. 121 (2), 55–64 (Transactions of the Institution of Mining and Metallurgy, Section B).

Agnihotri, R., Chauk, S., Mahuli, S., Fan, L.-S., 1998. Selenium removal using Ca-based sorbents: reaction kinetics. Environ. Sci. Technol. 32, 1841–1846. http://dx.doi.org/10.1021/es971119j.

Armstroff, A., 2004. Geochemical significance of biomarkers in paleozoic coals. Doctoral thesis (Ph.D). Technischen Universität Berlin. http://dx.doi.org/10.14279/depositonce-818.

Armstrong, J.A., Parnell, J., Bullock, L.A., Perez, M., Boyce, A.J., Feldmann, J., 2018. Tellurium, selenium and cobalt enrichment in Neoproterozoic black shales, Gwna Group, UK: deep marine trace element enrichment during the Second Great Oxygenation Event. Terra Nova 30, 244–253. http://dx.doi.org/10.1111/ter.12331.

Arthurton, R.S., Gutteridge, P., Nolan, S.C., 1989. The role of tectonics in Devonian and carboniferous sedimentation in the British isles. Occas. Publ. Yorks. Geol. Soc.(6).

Banks Group, 2010. Shotton Borehole Locations. Internal Report HJB/289/387.

Banks Group, 2018. Shotton. https://www.banksgroup.co.uk/projects/mining/shotton/ (Accessed: 15/03/2018).

Bloodworth, A.J., Harrison, D.J., Cameron, D.G., Holloway, S., Linley, K.A., Hough, E., 2000. Northumberland Tyne and wear mineral resources (map) scale 1:100,000. British Geol. Surv License Number GD272191/2000, Ref. No. WF/00/5.

Bottrell, S.H., Louie, P.K.K., Timpe, R.C., Hawthorne, S.B., 1994. The use of stable sulfur isotope ratio analysis to assess selectivity of chemical analyses and extractions of forms of sulfur in coal. Fuel 73 (10), 1578–1582. http://dx.doi.org/10.1016/0016-2361(94)90135-X.

Bouch, J.E., Naden, J., Shepherd, T.J., McKervey, J.A., Young, B., Benham, A.J., Sloane, H.J., 2006. Direct evidence of fluid mixing in the formation of stratabound Pb–Zn–Ba–F mineralisation in the Alston Block, North Pennine Orefield (England). Mineral. Deposita 41, 821–835. http://dx.doi.org/10.1007/s00126-006-0093-3.

Bragg, L.J., Oman, J.K., Tewalt, S.J., Oman, C.L., Rega, N.H., Washington, P.M., Finkelman, R.B., 1998. U.S. Geological Survey Coal Quality (COALQUAL) Database: Version 2.0. US Geological Survey Open File Report. pp. 97–134 (CD-ROM).

Brown, R.D., 2000. Selenium and tellurium. In: U.S. Geological Survey Minerals Yearbook. U.S. Geological Survey, Reston, VA, USA, pp. 1–8.

Bullock, L.A., Parnell, J., 2017. Selenium and molybdenum enrichment in uranium roll-front deposits of Wyoming and Colorado, USA. J. Geochem. Explor. 180, 101–112. http://dx.doi.org/10.1016/j.gexplor.2017.06.013.

Bullock, L.A., Parnell, J., Perez, M., Feldmann, J., 2017. Tellurium enrichment in Jurassic coal, Brora, Scotland. Fortschr. Mineral. 7 (12), 231. http://dx.doi.org/10.3390/min7120231.

Bullock, L.A., Parnell, J., Feldmann, J., Armstrong, J.A., Henn, A.S., Mesko, M.F., Mello, P.A., Flores, E.E., 2018a. Selenium and tellurium concentrations of British coals. Geol. J. 2018, 1–11. http://dx.doi.org/10.1002/gj.3238.

Bullock, L.A., Parnell, J., Perez, M., Boyce, A., Feldmann, J., Armstrong, J.A., 2018b. Multi-stage pyrite genesis and epigenetic selenium enrichment of Greenburn coals (East Ayrshire). Scott. J. Geol. 54, 37–49. http://dx.doi.org/10.1144/sjg2017-010.

Burnett, R.D., 1987. Regional maturation patterns for late Visean (carboniferous, Dinantian) rocks of northern England based on mapping of conodont colour. Irish J. Earth Sci. 8 (2), 165–185. https://www.jstor.org/stable/30002529.

Cann, J.R., Banks, D.A., 2001. Constraints on the genesis of the mineralization of the Alston Block, Northern Pennine Orefield, northern England. Proc. Yorks. Geol. Soc. 53, 187–196. http://dx.doi.org/10.1144/pygs.53.3.187.

Carter, J.A., Walker, R.L., Sites, J.R., 1975. Trace impurities in fuels by isotope dilution mass spectrometry. In: Babu, S.P. (Ed.), Trace Elements in Fuel Symposium, 1973. 141. pp. 74–83. Washington, D.C. American Chemical Society Advances in Chemistry Series. https://doi.org/10.1021/ba-1975-0141.ch007.

Cheng, J., 1980. The preliminary investigation report of selenium intoxication in Ziyang County of Shanxi Province. J. Shanxi Agric. Sci. 6, 17.

Clark, J., Zingaro, R.A., Irgolic, K.J., McGinley, N.N., 1980. Arsenic and selenium in Texas lignite. Int. J. Environ. Anal. Chem. 7, 295–314. https://doi.org/10.1080/03067318008071492.

Coleman, S.L., Bragg, L.J., Finkelman, R.B., 1993. Distribution and mode of occurrence of selenium in US coals. Environ. Geochem. Health 15, 215–227. http://dx.doi.org/10.1007/BF00146745.

Dai, S., Finkelman, R.B., 2018. Coal as a promising source of critical elements: progress and future prospects. Int. J. Coal Geol. 186, 155–164. http://dx.doi.org/10.1016/j.coal.2017.06.005.

Dai, S., Ren, D., Zheng, J., Hou, X., 2003. Concentrations and origins of platinum group elements in Late Paleozoic coals of China. Int. J. Coal Geol. 55, 59–70. http://dx.doi.org/10.1016/S0166-5162(03)00079-X.

Dai, S., Ren, D., Chou, C.-L., Li, S., Jiang, Y., 2006. Mineralogy and geochemistry of the no. 6 coal (Pennsylvanian) in the Junger Coalfield, Ordos Basin, China. Int. J. Coal Geol. 66, 253–270. http://dx.doi.org/10.1016/j.coal.2005.08.00.

Dai, S., Li, D., Choi, C.-L., Zhao, L., Zhang, Y., Ren, D., Ma, Y., Sun, Y., 2008. Mineralogy and geochemistry of boehmite-rich coals: new insights from the Haerwusu Surface Mine, Jungar Coalfield, Inner Mongolia, China. Int. J. Coal Geol. 74, 185–202. http://dx.doi.org/10.1016/j.coal.2008.01.00.

Dai, S., Ren, D., Chou, C.-L., Finkelman, R.B., Seredin, V.V., Zhou, Y., 2012. Geochemistry of trace elements in Chinese coals: a review of abundances, genetic types, impacts on human health, and industrial utilization. Int. J. Coal Geol. 94, 3–21. http://dx.doi.org/10.1016/j.coal.2011.02.003.

Dai, S., Seredin, V.V., Ward, C.R., Hower, J.C., Xing, Y., Zhang, W., Song, W., Wang, P., 2015a. Enrichment of U–Se–Mo–Re–V in coals preserved within marine carbonate successions: geochemical and mineralogical data from the late Permian guiding coalfield, Guizhou, China. Mineral. Deposita 50, 159–186. http://dx.doi.org/10.1007/s00126-014-0528-1.

Dai, S., Yang, J., Ward, C.R., Hower, J.C., Liu, H., Garrison, T.M., French, D., O'Keefe, J.M.K., 2015b. Geochemical and mineralogical evidence for a coal-hosted uranium deposit in the Yili Basin, Xinjiang, northwestern China. Ore Geol. Rev. 70, 1–30. http://dx.doi.org/10.1016/j.oregeorev.2015.03.010.

Dai, S., Xie, P., Jia, S., Ward, C.R., Hower, J.C., Yan, X., French, D., 2017. Enrichment of U-Re-V-Cr-Se and rare earth elements in the Late Permian coals of the Moxinpo Coalfield, Chongqing, China: genetic implications from geochemical and mineralogical data. Ore Geol. Rev. 80, 1–17. http://dx.doi.org/10.1016/j.oregeorev.2016.06.015.

Dai, S., Yan, X., Ward, C.R., Hower, J.C., Zhao, L., Wang, X., Zhao, L., Ren, D., Finkelman, R.B., 2018a. Valuable elements in Chinese coals: a review. Int. Geol. Rev. 60, 590–620. http://dx.doi.org/10.1080/00206814.2016.1197802.

Dai, S., Zheng, X., Wang, X., Finkelman, R.B., Jiang, Y., Ren, D., Yan, X., Zhou, Y., 2018b. Stone coal in China: a review. Int. Geol. Rev. 60, 736–753. http://dx.doi.org/10.1080/00206814.2017.1378131.

Diaz-Somoano, M., Martinez-Tarazona, M.R., 2004. Retention of arsenic and selenium compounds using limestone in a coal gasification flue gas. Environ. Sci. Technol. 38, 899–903. http://dx.doi.org/10.1080/00206814.2017.1378131.

Diehl, S.F., Goldhaber, M.B., Koenig, A.E., Lowers, H.A., Ruppert, L.F., 2012. Distribution of arsenic, selenium, and other trace elements in high pyrite Appalachian coals: evidence for multiple episodes of pyrite formation. Int. J. Coal Geol. 94, 238–249. http://dx.doi.org/10.1016/j.coal.2012.01.015.

Ding, Z., Zheng, B., Long, J., Belkin, H.E., Finkelman, R.B., Chen, C., Zhou, D., Zhou, Y., 2001. Geological and geochemical characteristics of high arsenic coals from endemic arsenosis areas in southwestern Guizhou Province, China. Appl. Geochem. 16, 1353–1360. http://dx.doi.org/10.1016/S0883-2927(01)00049-X.

Dreher, G.B., Finkelman, R.B., 1992. Selenium mobilization in a surface coal mine, Powder River basin, Wyoming, U.S.A. Environ. Geol. Water Sci. 19 (3), 155–167. http://dx.doi.org/10.1007/BF01704083.

Dunham, K.C., 1988. Pennine mineralisation in depth. Proc. Yorks. Geol. Soc. 47, 1–12. http://dx.doi.org/10.1144/pygs.47.1.1.

Dunoyer de Segonzac, G., 1970. The transformation of clay minerals during diagenesis and low-grade metamorphism: a review. Sedimentology 15, 281–346. http://dx.doi.org/10.1111/j.1365-3091.1970.tb02190.x.

Emsbo, P., Hofstra, A.H., Lauha, E.A., Griffin, G.L., Hutchinson, R.W., John, D.A., Theodore, T.G., 2003. Origin of high-grade gold ore, source of ore fluid components, and genesis of the Meikle and neighboring Carlin-type deposits, northern Carlin Trend, Nevada. Econ. Geol. Spec. Publ. 98, 1069–1105. http://dx.doi.org/10.2113/gsecongeo.98.6.1069.

Fiene, F.L., Kuhn, J.K., Gluskoter, H.J., 1979. Mineralogic affinities of trace elements in coal. In: Rogers, S.E., Lemmon Jr.A.W. (Eds.), Symp. on Coal Cleaning to Achieve Energy and Environ. Coals. Proc. vol. 1. EPA, Washington, D.C., pp. 29–58 Rep. EPA-600/7-79-098a.

Finkelman, R.B., 1980. Modes of Occurrence of Trace Elements in Coal. PhD thesis. University of Maryland.

Finkelman, R.B., Stanton, R.W., Blaine Cecil, C., Minkin, J.A., 1979. Modes of occurrence of selected trace elements in several Appalachian coals. In: Conference: 177. National Meeting of the American Chemical Society, Honolulu, HI, USA, 1 Apr 1979. 24. American Chemical Society Division of Fuel Chemistry, pp. 1.

Finkelman, R.B., Orem, W., Castranova, V., Tatu, C.A., Belkin, H.E., Zheng, B., Lerch, H.E., Maharaj, S.V., Bates, A.L., 2002. Health impacts of coal and coal use: possible solutions. Int. J. Coal Geol. 50, 425–443. http://dx.doi.org/10.1016/S0166-5162(02)00125-8.

Foscolos, A.E., Goodarzi, F., Koukouzas, C.N., Hatziyiannis, G., 1989. Reconnaissance study of mineral matter and trace elements in Greek lignites. Chem. Geol. 76, 107–130. http://dx.doi.org/10.1016/0009-2541(89)90131-9.

Gayer, R.A., Pesek, L., Sykorova, J., Valterova, J., 1996. Coal clasts in the upper Westphalian sequence of the South Wales coal basin: implications for the timing of maturation and fracture permeability. In: Gayer, R.A., Harris, I. (Eds.), Coalbed Methane and Coal Geology. 109. Geological Society, London, pp. 103–120. Special Publications. https://doi.org/10.1144/GSL.SP.1996.109.01.08.

Gentzis, T., Goodarzi, F., Foscolos, A.E., 1997. Geochemistry and mineralogy of Greek lignites from the Ioannina Basin. Energy Sources 19, 111–128. http://dx.doi.org/10.1080/00908319708908837.

Ghosh-Dastidar, A., Mahuli, S., Agnihotri, R., Fan, L.-S., 1996. Selenium capture using sorbent powders: mechanism of sorption by hydrated lime. Environ. Sci. Technol. 30, 447–452. http://dx.doi.org/10.1021/es950129m.

Goldhaber, M.B., Irwin, E.R., Atkins, J.B., Lee, R., Zappia, H., Black, D.D., Finkelman, R.B., 2000. Environmental impact of elevated arsenic in Southern Appalachian Basin coals. Metal Ions Biol. Med. 6, 38–40.

Goldschmidt, V.M., 1943. The Occurrence of Rare Elements in Coal Ashes (Published Lecture to British Coal Utilisation Research Association (BCURA), 8th May, 1943).

Goodarzi, F., Swaine, D.J., 1993. Behaviour of Boron in coal during natural and industrial combustion processes. Energy Sources 15, 609–622. http://dx.doi.org/10.1080/00908319308909052.

Granger, H.C., Warren, C.G., 1978. Some speculations on the genetic geochemistry and hydrology of roll-type uranium deposits. In: 30th Annual Conference, Wyoming Geological Association Guidebook, pp. 349–361.

Harshman, E.N., 1966. Genetic implications of some elements associated with uranium deposits, Shirley Basin, Wyoming. In: Geological Survey Research 1966. U.S. Geological Survey Professional Paper 550-C, pp. C167–C173.

Hatch, J.R., Gluskoter, H.J., Lindahl, P.C., 1976. Sphalerite in coals from the Illinois Basin. Econ. Geol. 71, 613–624. http://dx.doi.org/10.2113/gsecongeo.71.3.613.

He, B., Liang, L., Jiang, G., 2002. Distributions of arsenic and selenium in selected Chinese coal mines. Sci. Total Environ. 296, 19–26. http://dx.doi.org/10.1016/S0048-9697(01)01136-6.

Hendry, M.J., Biswas, A., Essilfie-Dughan, J., Chen, N., Day, S.J., Barbour, S.L., 2015. Reservoirs of Selenium in coal waste rock: Elk Valley, British Columbia, Canada. Environ. Sci. Technol. 49, 8236–8828. http://dx.doi.org/10.1021/acs.est.5b01246.

Henn, A.S., Rondan, F.S., Mesko, M.F., Mello, P.A., Perez, M., Armstrong, J.A., Bullock, L.A., Parnell, J., Feldmann, F., Flores, E.M.M., 2018. Determination of Se at low concentration in coal by collision/reaction cell technology inductively coupled plasma mass spectrometry. Spectrochim. Acta B At. Spectrosc. 143, 48–54. http://dx.doi.org/10.1016/j.sab.2018.02.014.

Hofmann, B.A., 1991. Mineralogy and geochemistry of reduction spheroids in red beds. Mineral. Petrol. 44, 107–124. http://dx.doi.org/10.1007/BF01167103.

Howard, J.H., 1977. Geochemistry of selenium: formation of ferroselite and selenium behavior in the vicinity of oxidizing sulfide and uranium deposits. Geochim. Cosmochim. Acta 41, 1665–1678. http://dx.doi.org/10.1016/0016-7037(77)90176-4.

Hower, J.C., Robertson, J.D., 2003. Clausthalite in coal. Int. J. Coal Geol. 53, 221–225. http://dx.doi.org/10.1016/S0166-5162(03)00022-3.

Jackson, I., Lawrence, D.J.D., Frost, D.V., 1985. Geological notes and local details for sheet NZ 27 (Cramlington, Killingworth and Wide Open). Brit. Geol. Surv. 43. http://nora.nerc.ac.uk/id/eprint/510153/1/WADM85014.pdf Newcastle upon Tyne.

Jin, R., Zhao, K., Pu, X., Zhang, M., Cai, F., Yang, X., Kin, H., Zhao, Y., 2016. Structural and photovoltaic properties of FeSe$_2$ films prepared by radio frequency magnetron sputtering. Mater. Lett. 179, 179–181. http://dx.doi.org/10.1016/j.matlet.2016.05.087.

Keith, M., Smith, D.J., Jenkin, G.R.T., Holwell, D.A., Dye, M.D., 2017. A review of Te and Se systematics in hydrothermal pyrite from precious metal deposits: insights into ore-forming processes. Ore Geol. Rev. 96, 269–282. http://dx.doi.org/10.1016/j.oregeorev.2017.07.023.

Ketris, M.P., Yudovich, Y.E., 2009. Estimations of Clarkes for carbonaceous biolithes: world averages for trace element contents in black shales and coals. Int. J. Coal Geol. 78, 135–148. http://dx.doi.org/10.1016/j.coal.2009.01.002.

Kolker, A., Panov, B.S., Panov, Y.B., Landa, E.R., Conko, K.M., Korchemagin, V.A.,

Shendrik, T., McCord, J.D., 2009. Mercury and trace element contents of Donbas coals and associated mine water in the vicinity of Donetsk, Ukraine. Int. J. Coal Geol. 79, 83–91. http://dx.doi.org/10.1016/j.coal.2009.06.003.

Kostova, I., Petrov, O., Kortenski, J., 1996. Mineralogy, geochemistry and pyrite content of Bulgarian subbituminous coals, Pernik Basin. In: Gayer, R., Harris, I. (Eds.), Coalbed Methane and Coal Geology. Geological Society Special Publication. 109. pp. 301–314.

Lakin, H.W., Davidson, D.F., 1973. Selenium. In: Brobst, D.A., Pratt, W.A. (Eds.), United States Mineral Resources. U.S. Geological Survey Professional Paper 820. pp. 573–576.

Leeder, M.R., McMahon, A.H., 1988. Upper Carboniferous (Silesian) basin subsidence in northern Britain. In: Besly, B.M., Kelling, G. (Eds.), Sedimentation in a Synorogenic Basin Complex: The Upper Carboniferous of Northwest Europe. Blackie and Son, Glasgow, pp. 43–52.

Lei, W., 2012. Selenium in Chinese Coal: Distribution, Mode and Occurrence and Environmental Geochemistry. PhD thesis. City University of Hong Kong.

Lemly, A.D., 2004. Aquatic selenium pollution is a global environmental safety issue. Ecotoxicol. Environ. Saf. 59, 44–56. http://dx.doi.org/10.1016/S0147-6513(03)00095-2.

Li, S., Zhao, L., 2007. Geochemistry and origin of lead and selenium in the no. 6 coal from the Junger Coalfield, North China. Energ. Explor. Exploitation 25 (3), 175–184. http://dx.doi.org/10.1260/014459807782009150.

Lin, R., Soong, T., Granite, E.J., 2018. Evaluation of trace elements in U.S. coals using the USGS COALQUAL database version 3.0. Part II: non-REY critical elements. Int. J. Coal Geol. 192, 39–50. http://dx.doi.org/10.1016/j.coal.2018.04.005.

Liu, G., Zheng, L., Zhang, Y., Qi, C., Chen, Y., Peng, Z., 2006. Distribution and mode of occurrence of As, Hg and Se and Sulfur in coal Seam 3 of the Shanxi Formation, Yanzhou Coalfield, China. Int. J. Coal Geol. 71, 371–385. http://dx.doi.org/10.1260/014459807782009150.

Liu, G., Yang, Z., Yan, X., Ji, D., Yang, Y., Hu, L., 2015. Modes of occurrence of highly-elevated trace elements in superhigh-organic-sulfur coals. Fuel 156, 190–197. http://dx.doi.org/10.1016/j.fuel.2015.04.034.

López-Antón, M., Díaz-Somoano, M., Fierro, J., Martínez-Tarazona, M., 2007. Retention of arsenic and selenium compounds present in coal combustion and gasification flue gases using activated carbons. Fuel Process. Technol. 88, 799–805. http://dx.doi.org/10.1016/j.fuproc.2007.03.005.

Lussier, C., Veiga, V., Baldwin, S., 2003. The geochemistry of selenium associated with coal waste in the Elk River Valley, Canada. Environ. Geol. 44, 905–913. http://dx.doi.org/10.1007/s00254-003-0833-y.

Mao, D., Su, H., Wang, Y., Luo, G., 1988. Preliminary study of selenium intoxication caused by weathering and burning of high selenium carbonaceous shale. J. Chin. Endemic Dis. 7, 297–299. http://dx.doi.org/10.1016/j.fuproc.2007.03.005.

Mao, D., Su, H., Yan, L., Wang, Y., Yu, X., 1990. Investigation and analysis of endemic selenois in Exi Autonomous Prefecture of Hubei province. Chin. J. Endemiol. 9, 311–314.

McDonald, L.E., Strosher, M.M., 1998. Selenium mobilization from surface coal mining in the Elk River Basin, British Columbia: a survey of water, sediment and biota. In: Pollution Prevention Ministry of Environment, Lands and Parks Report, Kootenay Region, Canbrook, British Columbia.

McKay, J.L., Longstaffe, F.J., 2003. Sulphur isotope geochemistry of pyrite from the Upper Cretaceous Marshybank Formation, Western Interior Basin. Sediment. Geol. 157, 175–195. http://dx.doi.org/10.1016/S0037-0738(02)00233-6.

Mills, D.A.C., Holliday, D.W., 1998. Geology of the district around Newcastle upon Tyne. In: Gateshead Consett. Memoir 1:50,000 Geological Sheet 20. British Geological Survey.

Min, M., Xu, H., Chen, J., Fayek, M., 2005. Evidence of uranium biomineralization in sandstone-hosted roll-front uranium deposits, northwestern China. Ore Geol. Rev. 26, 198–206. http://dx.doi.org/10.1016/j.oregeorev.2004.10.003.

National Coal Board Archive, 2011. The Northumberland Coalfield. Archived via. https://web.archive.org/web/20110719144206/http://www.cmhrc.pwp.blueyonder.co.uk/nblandcf.htm updated, Accessed: 15/03/2018.

Northrop, H.R., Goldhaber, M.B., 1990. Genesis of the tabular-type vanadium–uranium deposits of the Henry Basin, Utah. Econ. Geol. 85, 215–269. http://dx.doi.org/10.2113/gsecongeo.85.2.215.

Pals, D.W., Spry, P.G., Chryssoulis, S., 2003. Invisible gold and tellurium in arsenic rich pyrite from the Emperor gold deposit, Fiji: implications for gold distribution and deposition. Econ. Geol. 98, 479–493. http://dx.doi.org/10.2113/gsecongeo.98.3.479.

Parnell, J., Boyce, A.J., Hurst, A., Davidheiser-Kroll, B., Ponicka, J., 2013. Long term geological record of a global deep subsurface microbial habitat in sand injection complexes. Sci. Rep. 3 (1828). http://dx.doi.org/10.1038/srep01828.

Parnell, J., Brolly, C., Spinks, S., Bowden, S., 2016. Selenium enrichment in Carboniferous Shales, Britain and Ireland: problem or opportunity for shale gas extraction? Appl. Geochem. 66, 82–87. http://dx.doi.org/10.1016/j.apgeochem.2015.12.008.

Parnell, J., Perez, M., Armstrong, J.A., Bullock, L.A., Feldmann, J., Boyce, A.J., 2018a. Geochemistry and metallogeny of Neoproterozoic pyrite in oxic and anoxic sediments. Geochem. Perspect. Lett. 7, 12–16. http://dx.doi.org/10.7185/geochemlet.1812.

Parnell, J., Spinks, S., Brolly, C., 2018b. Tellurium and selenium in Mesoproterozoic red beds. Precambrian Res. 305, 145–150. http://dx.doi.org/10.1016/j.precamres.2017.12.022.

Pazand, K., 2015. Concentration and distribution of selenium in Iranian coals. Environ. Nanotechnol. Monit. Manag. 3, 55–60. http://dx.doi.org/10.1016/j.enmm.2014.12.003.

Pešek, J., Bencko, V., Sýkorová, I., Vašíček, M., Michna, O., Martínek, K., 2005. Some trace elements in coal of the Czech Republic, environment and health protection

implications. Cent. Eur. J. Public Health 13 (3), 153–158.

Plant, J.A., Bone, J., Voulvoulis, N., Kinniburgh, D.G., Smedley, P.L., Fordyce, F.M., Klinck, B., 2013. Arsenic and selenium. In: Treatise on Geochemistry, Second Edition. 11. Elsevier, Amsterdam, Netherlands, pp. 13–57.

Price, N.J., 1959. Mechanics of jointing in rocks. Geol. Mag. 96, 149–167.

Price, N.J., 1966. Fault and Joint Development in Brittle and Semi-Brittle Rock. Pergamon Press, New York.

Reynolds, R.L., Goldhaber, M.B., 1983. Iron disulfide minerals and the genesis of roll-type uranium deposits. Econ. Geol. 78, 105–120. http://dx.doi.org/10.2113/gsecongeo.78.1.105.

Riley, K.W., French, D.H., Lambropoulos, N.A., Farrell, O.P., Wood, R.A., Huggins, F.E., 2007. Origin and occurrence of selenium in some Australian coals. Int. J. Coal Geol. 72, 72–80. http://dx.doi.org/10.1016/j.coal.2006.12.010.

Rippon, J.H., 1996. Sand body orientation, palaeoslope analysis, and basin fill implications in the Westphalian A-C of Great Britain. J. Geol. Soc. 153, 881–900. http://dx.doi.org/10.1144/gsjgs.153.6.0881.

Rippon, J.H., 1998. The identification of syndepositionally active structures in the coal-bearing Upper Carboniferous of Great Britain. Proc. Yorks. Geol. Soc. 52, 73–93. http://dx.doi.org/10.1144/pygs.52.1.73.

Ruiz Cruz, M.D., Reyes, E., 1998. Kaolinite and dickite formation during shale diagenesis: isotopic data. Appl. Geochem. 13, 95–104. http://dx.doi.org/10.1016/S0883-2927(97)00056-5.

Seredin, V.V., Finkelman, R.B., 2008. Metalliferous coals: a review of the main genetic and geochemical types. Int. J. Coal Geol. 76, 253–289. http://dx.doi.org/10.1016/j.coal.2008.07.016.

Seredin, V.V., Dai, S., Sun, Y., Chekryzhov, I.Y., 2013. Coal deposits as promising sources of rare metals for alternative power and energy-efficient technologies. Appl. Geochem. 31, 1–11. http://dx.doi.org/10.1016/j.apgeochem.2013.01.009.

Simon, G., Kesler, S.E., Essene, E.J., 1997. Phase relations among selenides, sulfides, tellurides, and oxides: II. Applications to selenide-bearing ore deposits. Econ. Geol. 92, 468–484. http://dx.doi.org/10.2113/gsecongeo.92.4.468.

Song, C., 1989. A Brief Description of the Yutangba Sedimentary Type Se Mineralized Area in Southwestern Hubei. Mineral Deposits. 8. pp. 83–88.

Spears, D.A., 1961. Joints in the Whin sill and associated sediments in Upper Teesdale, Northern Pennines. Proc. Yorks. Geol. Soc. 33, 21–30. http://dx.doi.org/10.1144/pygs.33.1.21.

Spears, D.A., 2015. The geochemistry and mineralogy of high-S coals, with examples mainly from the East Pennines coalfield in Yorkshire and Nottinghamshire, UK: an overview. Proc. Yorks. Geol. Soc. 60, 204–226. http://dx.doi.org/10.1144/pygs2015-356.

Spears, D.A., 2017. The role of seawater on the trace element geochemistry of some UK coals and a tribute to Goldschmidt. Minerals 7 (148). http://dx.doi.org/10.3390/min7080148.

Spears, D.A., Amin, M.A., 1981. Geochemistry and mineralogy of marine and non-marine Namurian black shales from the Tansley Borehole, Derbyshire. Sedimentology 28, 407–417. http://dx.doi.org/10.1111/j.1365-3091.1981.tb01689.x.

Spears, D.A., Booth, C.A., 2002. The composition of size-fractionated pulverised coal and the trace element associations. Fuel 81, 683–690. http://dx.doi.org/10.1016/S0016-2361(01)00156-9.

Spears, D.A., Caswell, S.A., 1986. Mineral matter in coals: cleat minerals and their origin in some coals from the English Midlands. Int. J. Coal Geol. 6, 107–125. http://dx.doi.org/10.1016/0166-5162(86)90015-7.

Spears, D.A., Tewalt, S.J., 2009. The geochemistry of environmentally important trace elements in UK coals, with special reference to the Parkgate Coal in the Yorkshire – Nottinghamshire Coalfield, UK. Int. J. Coal Geol. 80, 157–166. http://dx.doi.org/10.1016/j.coal.2009.08.010.

Spears, D.A., Zheng, Y., 1999. Geochemistry and origin of elements in some UK coals. Int. J. Coal Geol. 38, 161–179. http://dx.doi.org/10.1016/S0166-5162(98)00012-3.

Spears, D.A., Manzanares-Papayanopoulus, L.I., Booth, C.A., 1999. The distribution and origin of trace elements in UK coal and the importance of pyrite. Fuel 78, 1671–1677. http://dx.doi.org/10.1016/S0016-2361(99)00114-3.

Spinks, S.C., Parnell, J., Still, J.W., 2014. Redox-controlled selenide mineralization in the Upper Old Red Sandstone. Scott. J. Geol. 50, 173–182. http://dx.doi.org/10.1144/sjg2013-014.

Spinks, S.C., Parnell, J., Bellis, D., Still, J., 2016. Remobilization and mineralization of selenium–tellurium in metamorphosed red beds: evidence from the Munster Basin, Ireland. Ore Geol. Rev. 72, 114–127. http://dx.doi.org/10.1016/j.oregeorev.2015.07.007.

Stillings, L.L., Schulz, K.J., 2017. Selenium. Chapter Q of In: DeYoung Jr.J.H., Seal IIR.R., Bradley, D.C. (Eds.), U.S. Geological Survey Professional Paper. Critical mineral resources of the United States - economic and environmental geology and prospects for future supply 1802. pp. Q1–Q55. http://dx.doi.org/10.3133/pp1802Q.

Stone, P., Millward, D., Young, B., Merritt, J.W., Clarke, S.M., McCormac, M., Lawrence, D.J.D., 2010. British Regional Geology: Northern England, Fifth edition. British Geological Survey, Keyworth, Nottingham.

Stricker, G.D., Ellis, M.S., 1999. Coal Quality and Geochemistry, Powder River Basin, Wyoming and Montana. US Geological Survey Professional Paper, 1625-A.

Su, H., Yan, L., Rao, S., Jian, X., Mao, D., 1990. Investigation of the cause of the origination of the environmental selenium and high selenium area in the Exi Autonomous Prefecture of Hubei Province. Environ. Sci. 11, 86–89.

Swaine, D.J., 1990. Trace Elements in Coal. Butterworth, London, UK.

Tanner, D., Henley, R.W., Mavrogenes, J.A., Holden, P., 2016. Sulfur isotope and trace element systematics of zoned pyrite crystals from the El Indio Au-Cu-Ag deposit, Chile. Contrib. Mineral. Petrol. 171 (4) 33-1-33-17. https://doi.org/10.1007/s00410-016-1248-6.

Tian, H., Shuai, Q., Xu, S., Bao, Z., Xie, S., 2014. Novel technology of preparation of crudes selenium from Serich stone coal. Earth Sci. 39 (7), 880–888.

Troshin, Y.P., Lomonosov, I.S., Lomonosova, T.K., Bryukhanova, N.N., Gvozdkov, A.N., Geletii, V.F., Petrov, L.L., Sandimirov, I.V., Spiridonov, A.M., Tkachenko, L.L., 2001. Geochemistry of the ore-bearing elements in sediments of the Cenozoic depressions, Baikal rift zone. In: Russian Geology and Geophysics c/c of Geologiia I Geofizica. 42. pp. 348–361.

Tucker, M.E., 2012. Sedimentary Petrology: An Introduction to the Origin of Sedimentary Rocks, Third edition. Blackwell Science Ltd., Malden, MA.

Turner, B.R., Richardson, D., 2004. Geological controls on the sulphur content of coal seams in the Northumberland Coalfield, Northeast England. Int. J. Coal Geol. 60, 169–196. http://dx.doi.org/10.1016/j.coal.2004.05.003.

UKERC UK Energy Research Centre, 2012. Energy Materials Availability Handbook. UK Energy Research Centre, London, UK.

Warwick, P.D., Crowley, S.S., Thomas, R.E., 1995. Distribution of HAPs trace elements in U.S. Gulf coast coals. In: Twelfth Annual International Pittsburgh Coal Conference Proceedings, pp. 1146–1150 Sept. 11–15.

Wei, C., Bai, Y., Deng, A., Bao, Y., 2016. Universal synthesis of air stable, phase pure, controllable FeSe$_2$ nanocrystals. Nanotechnology 27 (9pp), 165702. http://dx.doi.org/10.1088/0957-4484/27/16/165702.

White, R.N., Smith, J.V., Spears, D.A., Rivers, M.L., Sutton, S.R., 1989. Analysis of iron sulphides from U.K. coal by synchrotron radiation X-ray fluorescence. J. Inst. Fuel 68, 1480–1486. http://dx.doi.org/10.1016/0016-2361(89)90048-3.

Xiong, Y.L., 2003. Predicted equilibrium constants for solid and aqueous selenium species to 300 °C: applications to selenium-rich mineral deposits. Ore Geol. Rev. 23, 259–276. http://dx.doi.org/10.1016/S0169-1368(03)00038-6.

Xu, G., Hannah, J.L., Bingen, B., Georgiev, S., Stein, H.J., 2012. Digestion methods for trace element measurements in shales: paleoredox proxies examined. Chem. Geol. 324-325, 132–147. http://dx.doi.org/10.1016/j.chemgeo.2012.01.029.

Yang, L., Wang, Q., Bai, X., Deng, J., Hu, Y., 2018. Mapping of trace elements in coal and ash research based on a bibliometric analysis method spanning 1971–2017. Minerals 8, 89. http://dx.doi.org/10.3390/min8030089.

Yudovich, Y.E., Ketris, M.P., 2005. Arsenic in coal: a review. Int. J. Coal Geol. 61, 141–196. http://dx.doi.org/10.1016/j.coal.2004.09.003.

Yudovich, Y.E., Ketris, M.P., 2006. Selenium in coal: a review. Int. J. Coal Geol. 67, 112–126. http://dx.doi.org/10.1016/j.coal.2005.09.003.

Yudovich, Y.E., Ketris, M.P., 2015. Geochemistry of Coal: Occurrences and Environmental Impacts of Trace Elements. In: Riazi, M.R., Gupta, R. (Eds.), Coal Production and Processing Technology. CRC Press, Boka Raton.

Zheng, B.S., Hong, Y., Zhou, W., Xia, W., Su, H., Mao, D., Yan, L., Thornton, I., 1992. The Se-rich carbonaceous siliceous rock and endemic selenosis in southwest Hubei, China. Chin. Sci. Bull. 37, 1725–1729. http://dx.doi.org/10.1360/sb1992-37-20-1725.

Zheng, B.S., Ding, Z., Huang, R., 1999. Issues of health and disease relating to coal use in southwest China. Int. J. Coal Geol. 40, 119–132. http://dx.doi.org/10.1016/S0166-5162(98)00064-0.

Zhu, J.M., Johnson, T.M., Finkelman, R.B., Zheng, B.S., Sýkorová, I., Pešek, J., 2012. The occurrence and origin of selenium minerals in Se-rich stone coals, spoils and their adjacent soils in Yutangba, China. Chem. Geol. 330–331, 27–38. http://dx.doi.org/10.1016/j.chemgeo.2012.08.023.